Applied Mathematics and Computation 475 (2024) 128699

Contents lists available at ScienceDirect

Applied Mathematics and Computation

journal homepage: www.elsevier.com/locate/amc

A novel observer-based neural-network finite-time output control for high-order uncertain nonlinear systems

Hoai Vu Anh Truong [a], Van Du Phan [b], Duc Thien Tran [c], Kyoung Kwan Ahn [d,*]

[a] Department of Mechanical Engineering, Pohang University of Science and Technology, Gyeongbuk 37673, South Korea
[b] School of Engineering and Technology, Vinh University, Nghe An 43100, Viet Nam
[c] Automatic Control Department, Ho Chi Minh City University of Technology and Education, Ho Chi Minh City 700000, Viet Nam
[d] School of Mechanical Engineering, University of Ulsan, Ulsan 44610, South Korea

ARTICLE INFO

Keywords:
Backstepping control
Nonlinear systems
Radial basis function neural network (RBFNN)
State observer
Disturbance observer
Finite-time control

ABSTRACT

Due to the difficulty encountered in dealing with unstructured system dynamics with unmeasured system state variables, this paper presents a novel observer-based neural network finite-time output control strategy for general high-order nonlinear systems (HNSs). The suggested technique is performed based on the backstepping-like control (BSC) scheme with a hybrid nonlinear disturbance-state observer and norm estimation-based radial basis function neural network (RBFNN). This helps not only reduce the number of estimated parameters but also relax the restriction of using inequality when exploiting the norm estimation concept in a conventional way; thus, retaining the same properties of the original system. Therefore, an observer-based finite-time output feedback control is established to deal with the unstructured dynamical behaviors and satisfying the output tracking regulation with the semi-global practically finite-time stability (SGPFS) guaranteed for the closed-loop system. The effectiveness and workability of the proposed algorithm is verified by a numerical simulation on a specific practical application.

1. Introduction

Requirement of precise output tracking performance, with stability and robustness, for high-order nonlinear systems (HNSs) in practical applications has evoked an interesting topic of control development. Several attractive algorithms have been carried out [1–7], based on the structure of backstepping-like control (BSC) as its advantage of stabilization via recursive processes [8]. However, existing problems of unmeasured state variables with parametric uncertainties, and unknown system dynamics in HNS have brought certain obstacles in developing advanced control strategies to satisfy the system output qualification with the robustness guaranteed.

For the first concern, several techniques were presented such as state observer, high-gain observer, extended state observer (ESO) [9–13], and so on. For example, Yao et al. developed an ESO for an electro-hydraulic system (EHS) to not only observe the mismatched and matched uncertainties but system state of velocity also [9]. In [10–12], the authors considered the case where only system output was measurable; thus, an ESO was constructed to obtain both an unmeasured state and matched uncertainty. Developed to general high-order nonlinear systems, the authors in [13] expressed ESO to cope with effects of both mismatched and matched uncertainties. These approaches can estimate unmeasured system states or unmeasurable variables based on the output. However, the literature did not consider the case of unknown dynamical behavior. Practically, time-varying unknown dynamics makes a certain influence on

* Corresponding author.
E-mail address: kkahn@ulsan.ac.kr (K.K. Ahn).

https://doi.org/10.1016/j.amc.2024.128699
Received 28 May 2023; Received in revised form 12 January 2024; Accepted 20 March 2024
Available online 17 April 2024

estimation qualification.

Regarding the above remaining, observer-based approximation techniques have been proposed, such as using fuzzy logic systems (FLS) or radial basis function neural networks (RBFNN)-based universal approximator [8,14–36], to deal with un-modeled or unstructured dynamics and parametric uncertainties due to their capability of approximating smooth function. Numerous observer-based approximation strategies have been successfully applied to practical applications such as hydraulic systems [14], pneumatic artificial muscle [15], robotic manipulators [8,16–18], and other HNS [34–36] with various advanced techniques combined. For example, in [19,20], the authors developed an observer-based adaptive control with RBFNN operator for non-strict feedback systems to deal with partially unknown dynamics and unmeasured state variables. In [21], an event-triggered technique with a state observer was combined for an uncertain strict feedback system subjected to actuator fault. The author in [22] applied a state observer-based fuzzy logic control for an uncertain nonlinear system with unmeasured state estimation and fault detection. More results that show the effectiveness of the RBFNN or FLS to cope with unknown dynamical behavior can be further referred to [23–36]. Essentially, the approximated output qualification depends on a number of nodes (or elements of unknown weighting vector in other words) in the hidden layers of the mechanism. To improve the approximation accuracy, the number of nodes should be increased; however, this certainly brings a time-consuming and burden computation due to the step-by-step when employing the backstepping-based method. To reduce the number of estimated parameters, a concept of using a Euclidean norm of weighting vector estimation has been alternatively introduced. In [37,38], the authors constructed the NN-like approximator with a norm of weighting vector estimation for strict feedback nonlinear systems. In [39–41] the authors extended this approach for non-strict feedback nonlinear systems concerning problems of state constraint, input saturation, and so forth. In [42], Liu et al. studied a decentralized NN-based adaptive finite-time control for general large-scale systems with state constraints. The literature indicates the effectiveness of using norm estimation in the control design to take the place of the conventional RBFNN approach. Moreover, by using this way, finite-time control can be formulated. Nevertheless, there is no report on using this approach with the state estimation for control development in HNS. Regarding the literature on using the RBFNN approximator with norm estimation, this technique is constructed based on the theory of inequality. In this manner, the control signals and adaptive laws are determined in such a way that they always bound the system dynamics. Unfortunately, by following this manner, unstructured dynamics, or information of approximated term if utilizing conventional RBFNN, cannot be reconstructed as a result. With the approximated unstructured dynamics omitted, unmeasured system states cannot be accurately observed because of the couple between the system states and system dynamics; thus, bringing another issue for the states estimation and further developments. Although results in [14] and [39] mentioned the norm estimation in the design of the adaptive law with a state observer, this brought a redundancy whereby both the weighting vector and its norm needed to be estimated. Solving the difficulty when combining the norm estimation technique with the state observer is the main motivation for this paper.

Besides, it should be mentioned that the BSC has been regarded as an efficient tool to construct controllers for HNSs. Accordingly, the command filter (CF) technique was also involved to not only obtain their derivative in the recursive progress but also help smoothen the intermediate virtual control signals and filter out noise; thus, addressing the complexity explosion, inherently existing in the BSC design. The effectiveness of this algorithm for practical applications has been verified in the literature [43–46]. However, with the former of norm estimation, the system dynamics could not be reconstructed; thus, restricting the use of the CF approach due to the infeasibility of the state estimation. Unfortunately, this issue has yet to be clarified from control developments.

Therefore, it is the purpose of this paper to construct an observer-based neural network finite-time output feedback control for general HNSs suffered from unknown systems dynamics and only output measured. To the best of our knowledge, this is the first time the RFNN, with the norm estimation used, is integrated with a hybrid nonlinear state and disturbance observer (NSDO) and CF approach. The key innovations of this scope are:

1) Completely different from the literature, this work first time deploys the norm estimation concept in a new way to facilitate the control development with other advanced techniques, by which the inequality constraint is relaxed but still keeps the same properties of the original system,
2) Due to only output measured, an NDSO-based RBFNN is accordingly employed for not only system states but also lumped disturbances and uncertainties estimation for the system dynamical behaviors compensation, which has escaped the attractiveness in the literature,
3) With the new-way approximation and estimation results, an observer-based NN finite time control is designed with the CF approach involved to deal with the complexity explosion in BSC design and achieve the system output regulation. The semi-global practically finite-time stability (SGPFS) of the closed-loop system is theoretically proven with Lyapunov theorem.

The rest of the paper remains: Section 2 describes system dynamics with preliminaries for control implementations. In Section 3, the new system reformulation is explained based on a new RBFNN-approximator with the NDSO. Thus, in Section 4, the proposed control algorithm is expressed with closed-loop system stability proof. Section 5 verifies the effectiveness of the proposed control scheme through a simulation of a specific electro-hydraulic system (EHS). Finally, the potential for control development with more advanced techniques is discussed in Section 6.

2. System descriptions and preliminaries

2.1. System descriptions

Consider an n-order nonlinear system as

$$\begin{cases} \dot{x}_k = f_k(\mathbf{x}) + g_k(\bar{\mathbf{x}}_k)x_{k+1} + d_k, \ (k = 1, ..., n-1) \\ \dot{x}_n = f_n(\mathbf{x}) + g_n(\bar{\mathbf{x}}_n)u + d_n \\ y = x_1 \end{cases}, \tag{1}$$

where $\mathbf{x} = (x_1, x_2, \ldots, x_n)^T$; $\bar{\mathbf{x}}_k = (x_1, x_2, \ldots, x_k)^T$; $f_k(\mathbf{x})$ is unknown but bounded and smooth function which is performed as $f_k(\mathbf{x}) = \boldsymbol{\Xi}_k^{*T}\boldsymbol{\varphi}_k(\mathbf{x})$ with $\boldsymbol{\Xi}_k^* = \begin{pmatrix} \xi_{k,1} & \xi_{k,2} & \cdots & \xi_{k,N_k} \end{pmatrix}^T \in \mathbb{R}^{N_k}$ being an unknown but bounded ideal vector of N_k elements and $\boldsymbol{\varphi}_k(\mathbf{x}) \in \mathbb{R}^{N_k}$ being a known-structured vector that includes system states; d_k and d_n represent for, in turn, mismatched and matched disturbances, $g_k(\bar{\mathbf{x}}_k) = g_k(x_1, x_2, \ldots, x_k)$ are known smooth functions with $g_k(\bar{\mathbf{x}}_k) > 0 \ \forall k$; and u is the control input signal. For the sake of simplicity, hereafter, we abbreviate $g_k(\bar{\mathbf{x}}_k)$ by g_k.

As the system state variables are unmeasured, except measured x_1, system (1) is rewritten as

$$\begin{cases} \dot{x}_k = \boldsymbol{\Xi}_k^{*T}\boldsymbol{\varphi}_k(\hat{\mathbf{x}}) + g_k x_{k+1} + d_k + e_k \\ \dot{x}_n = \boldsymbol{\Xi}_n^{*T}\boldsymbol{\varphi}_n(\hat{\mathbf{x}}) + g_n u + d_n + e_n \\ y = x_1 \end{cases}, \tag{2}$$

where $\hat{\mathbf{x}}$ is an estimation of $\mathbf{x}$ and $e_k = \boldsymbol{\Xi}_k^{*T}\boldsymbol{\varphi}_k(\mathbf{x}) - \boldsymbol{\Xi}_k^{*T}\boldsymbol{\varphi}_k(\hat{\mathbf{x}}), \ k = 1, \ldots, n$.

Besides, to facilitate the control and state observer implementations and stability proof, the following assumption is held:

Assumption 1. [10]: The nonlinear smooth functions $\boldsymbol{\Xi}_k^{*T}\boldsymbol{\varphi}_k(\mathbf{x})$ and $\boldsymbol{\Xi}_k^{*T}\boldsymbol{\varphi}_k(\hat{\mathbf{x}})$ is Lipschitz continuous that satisfies:

$$|e_k| = \left|\boldsymbol{\Xi}_k^{*T}\boldsymbol{\varphi}_k(\mathbf{x}) - \boldsymbol{\Xi}_k^{*T}\boldsymbol{\varphi}_k(\hat{\mathbf{x}})\right| \leq \sigma_k \| \mathbf{x} - \hat{\mathbf{x}} \|, \tag{3}$$

with σ_k being a constant.

2.2. Finite-time stability theorem

To facilitate finite-time stability, the following inequalities are introduced.

Lemma 1. [42]: *Regarding Young's inequality, the following condition holds:*

$$xy \leq \frac{\delta^a}{a}|x|^a + \frac{1}{b\delta^b}|y|^b, \tag{4}$$

where $\delta > 0$, $a, b > 1$ and$\frac{1}{a} + \frac{1}{b} = 1$. paper, $a = b = 2$ and $\delta = 1$ are selected.

Lemma 2. [41]: *For $\frac{1}{2} < \iota = p/q < 1$ with p, q being odd constants, and $\vartheta_k \in R$, $k = 1, 2, \ldots, n$, the following inequality is obtained:*

$$\left(\sum_{k=1}^{n} |\vartheta_k|\right)^{i} \leq \sum_{k=1}^{n} |\vartheta_k|^{\iota}. \tag{5}$$

Lemma 3. [32]: *Consider a nonlinear system $\dot{x} = f(x)$. If a continuous and smooth function $V(x)$ can be presented in the form of $\dot{V}(x) + \Gamma_1 V(x) + \Gamma_2 V^{\beta}(x) + C \leq 0$, with $\Gamma_1 > 0$, $\Gamma_2 > 0$, and $0 < \beta < 1$, then, the solution of $\dot{x} = f(x)$ is SGPFS, where the system-states' trajectory is semi-globally practically finite-time stable and converges to the neighborhood of the equilibrium in $t \geq t_0 + T_c$. Similar results and proof can be found in* [32,42]. *The finite-time convergence, T_c, is then determined as*

$$T_c \leq \max\left\{ t_0 + \frac{1}{\lambda_0\Gamma_1(1-\beta)}\ln\frac{\lambda_0\Gamma_1 V^{1-\beta}(t_0) + \Gamma_2}{\Gamma_2}, \ t_0 + \frac{1}{\Gamma_1(1-\beta)}\ln\frac{\Gamma_1 V^{1-\beta}(t_0) + \lambda_0\Gamma_2}{\lambda_0\Gamma_2} \right\}, \tag{6}$$

with $0 < \lambda_0 < 1$ and the function $V(x)$ is bounded by:

$$\lim_{t \to T_c} V(x) \leq \min\left\{ \frac{C}{(1-\lambda_0)\Gamma_1}, \left(\frac{C}{(1-\lambda_0)\Gamma_2}\right)^{\frac{1}{\beta}} \right\}. \tag{7}$$

Remark 1. Results inherited from Lemma 3 evoke a general form for the SGPFS, which provides faster convergence to the neighborhood of the equilibrium when the system state is far from this point. Besides, one can realize that if adopting $\Gamma_1 = 0$, or setting respective control gains to be zero in other words, the result in Lemma 3 becomes $\dot{V}(x) + \Gamma_2 V^{\beta}(x) + C \leq 0$, which is an original

structure of the finite-time control and if setting corresponding finite-time control gains to be zero, i.e., $\Gamma_2 = 0$, the closed-loop system is asymptotically stable with the system states being asymptotically converges to the neighborhood of the origin. Therefore, the SGPFS employed in this paper covers ordinary control schemes.

2.3. Command filter technique

To smoothen the virtual control signals and obtain its first derivative, the CF technique is conducted based on a first-order low-pass filter as

$$\varpi_{k,c}\dot{\chi}_{k,c} + \chi_{k,c} = \alpha_k. \tag{8}$$

where the virtual control signal α_k is of the input of the DSC, at step k; $\chi_{k,c}$ and $\dot{\chi}_{k,c}$ are the output of filtered intermediate virtual control and its derivative; respectively.

Lemma 4. [43]: *In case of noise existing, the tracking errors satisfy:*

$$\begin{cases} |\chi_{k,c} - \alpha_k| \le \varpi_k^u \\ |\dot{\chi}_{k,c} - \dot{\alpha}_k| \le \varpi_k^d \end{cases}, \tag{9}$$

if noise is bounded, with ϖ_k^u and ϖ_k^d being positive constants.

Remark 2. The condition introduced in Lemma (4) is required for the control law implementation. If noise is unbounded, the output x_1 cannot be measured, or x_1 is unobservable in other words. If x_1 is unobserved, then tracking error cannot be obtained and thus the virtual control signal α_k cannot be derived. Consequently, u cannot be designed and the system is uncontrollable as a result. Therefore, the condition of bounded noise is necessary to guarantee the observability and controllability of the system. Moreover, with this condition, the boundedness (9) can be satisfied, which facilitates the control implementation and stability proof of the closed-loop system.

3. System reformulation

3.1. Radial basis function neural network-based approximation

Due to the problem of the algebraic loop at step k, $\boldsymbol{\Xi}_k^{*T}\boldsymbol{\varphi}_k(\widehat{\mathbf{x}})$ is then presented through a calculation of k inputs as

$$\boldsymbol{\Xi}_k^{*T}\boldsymbol{\varphi}_k(\widehat{\mathbf{x}}) \leftarrow \boldsymbol{\Xi}_k^{*T}\boldsymbol{\varphi}_k(\widehat{\mathbf{x}}|\widehat{\overline{\mathbf{x}}}_k) = \boldsymbol{\Xi}_k^{*T}\boldsymbol{\varphi}_k(\widehat{\overline{\mathbf{x}}}_k), \tag{10}$$

where $\widehat{\overline{\mathbf{x}}}_k = (x_1, \widehat{x}_2, ..., \widehat{x}_k)^T$ is an estimated vector of $\overline{\mathbf{x}}_k$.

Thereby, there certainly exists an error:

$$\Delta_k = \boldsymbol{\Xi}_k^{*T}\boldsymbol{\varphi}_k(\widehat{\mathbf{x}}) - \boldsymbol{\Xi}_k^{*T}\boldsymbol{\varphi}_k(\widehat{\overline{\mathbf{x}}}_k). \tag{11}$$

Conventionally, the structure of the vector $\boldsymbol{\varphi}_k(\widehat{\overline{\mathbf{x}}}_k)$ is performed in the Gaussian basis function as

$$\begin{cases} \boldsymbol{\varphi}_k(\widehat{\overline{\mathbf{x}}}_k) = [\,\varphi_{k,1}(\widehat{\overline{\mathbf{x}}}_k) \quad \varphi_{k,2}(\widehat{\overline{\mathbf{x}}}_k) \quad ... \quad \varphi_{k,N_k}(\widehat{\overline{\mathbf{x}}}_k)\,]^T \\ \varphi_{k,j}(\widehat{\overline{\mathbf{x}}}_k) = \exp\left[-\dfrac{\left(\widehat{\overline{\mathbf{x}}}_k - \mathbf{c}_{k,j}\right)^T\left(\widehat{\overline{\mathbf{x}}}_k - \mathbf{c}_{k,j}\right)}{\left(2\mu_{k,j}\right)^2} \right] \end{cases}, \tag{12}$$

where $\mathbf{c}_{k,j}$ and $\mu_{k,j}$ are, in turn, the vector of the center and width of the Gaussian functions of each node in the hidden layer of the neural network. It is noteworthy that $\boldsymbol{\varphi}_k^T(\widehat{\overline{\mathbf{x}}}_k)\boldsymbol{\varphi}_k(\widehat{\overline{\mathbf{x}}}_k) \le N$.

Lemma 5. [47]: *For any positive integers $m > n > 0$, the following inequality for the basis function $\boldsymbol{\varphi}_k(\widehat{\overline{\mathbf{x}}}_n)$ holds:*

$$\| \boldsymbol{\varphi}_k(\widehat{\overline{\mathbf{x}}}_m) \|^2 \le \| \boldsymbol{\varphi}_k(\widehat{\overline{\mathbf{x}}}_n) \|^2 \le N. \tag{13}$$

In view of *Lemma 1*, the approximated term $f_k(\widehat{\overline{\mathbf{x}}}_k)$ in (10) is constrained by:

$$\boldsymbol{\Xi}_k^{*T}\boldsymbol{\varphi}_k(\widehat{\overline{\mathbf{x}}}_k) \le \frac{1}{2}\theta_k^*\boldsymbol{\varphi}_k^T(\widehat{\overline{\mathbf{x}}}_k)\boldsymbol{\varphi}_k(\widehat{\overline{\mathbf{x}}}_k) + \frac{1}{2}. \tag{14}$$

where $\theta_k^* = \| \boldsymbol{\Xi}_k^* \|^2$ is the Euclidean norm of the weighting vector $\boldsymbol{\Xi}_k^*$. Based on *Lemma 5* and inequality (14), the error Δ_k is constrained by $|\Delta_k| \le \overline{\Delta} = N\theta_k^* + 1$.

The original concept of the norm of weighting vector estimation is employed for the right-hand side of (14), where the norm θ_k^* or its

estimation is used in the derived control law. However, following this manner will completely omit the presence of unknown terms $\boldsymbol{\Xi}_k^{*T}\boldsymbol{\varphi}_k(\widehat{\mathbf{x}}_k)$, and thus restricting the observer implementation. Hence, to use the norm concept and also facilitate more advanced techniques development, the following assumption is introduced:

Assumption 2. There exists a time-varying bounded c_k^* such that:

$$\boldsymbol{\Xi}_k^{*T}\boldsymbol{\varphi}_k(\widehat{\mathbf{x}}_k) = \frac{1}{2}\theta_k^*\boldsymbol{\varphi}_k^T(\widehat{\mathbf{x}}_k)\boldsymbol{\varphi}_k(\widehat{\mathbf{x}}_k) + c_k^*. \tag{15}$$

Remark 3. The idea comes from the fact that the left-hand side (LHS) of (14) can be either positive or negative depending on the dynamical behaviors $\boldsymbol{\Xi}_k^{*T}\boldsymbol{\varphi}_k(\widehat{\mathbf{x}}_k)$ whereas the term $\frac{1}{2}\theta_k^*\boldsymbol{\varphi}_k^T(\widehat{\mathbf{x}}_k)\boldsymbol{\varphi}_k(\widehat{\mathbf{x}}_k)+\frac{1}{2}$ on the right-hand side (RHS) is non-negative, i.e., $\boldsymbol{\Xi}_k^{*T}\boldsymbol{\varphi}_k(\widehat{\mathbf{x}}_k) \le \left|\boldsymbol{\Xi}_k^{*T}\boldsymbol{\varphi}_k(\widehat{\mathbf{x}}_k)\right| \le \frac{1}{2}\theta_k^*\boldsymbol{\varphi}_k^T(\widehat{\mathbf{x}}_k)\boldsymbol{\varphi}_k(\widehat{\mathbf{x}}_k)+\frac{1}{2}$. Directly using inequality (14) restricts the use of observer in estimating unmeasured system states because what we deal with is the RHS of (14), not the original form on the LHS. Hence, there certainly exist a time-varying c_k^* to equalizes (14), as a result in (15). Thus, the constraint of $\boldsymbol{\Xi}_k^{*T}\boldsymbol{\varphi}_k(\widehat{\mathbf{x}}_k)$ is replaced by another way whereby inequality (14) still satisfies but the approximated term $\boldsymbol{\Xi}_k^{*T}\boldsymbol{\varphi}_k(\widehat{\mathbf{x}}_k)$ still complies with the norm estimation technique.

Hence, system (2) is rewritten to:

$$\begin{cases} \dot{x}_k = \frac{1}{2}\theta_k^*\boldsymbol{\varphi}_k^T(\widehat{\mathbf{x}}_k)\boldsymbol{\varphi}_k(\widehat{\mathbf{x}}_k) + g_k x_{k+1} + d_k + e_k + \Delta_k + c_k^* \\ \dot{x}_n = \frac{1}{2}\theta_n^*\boldsymbol{\varphi}_n^T(\widehat{\mathbf{x}})\boldsymbol{\varphi}_n(\widehat{\mathbf{x}}) + g_n u + d_n + e_n + \Delta_n + c_n^* \\ y = x_1 \end{cases}. \tag{16}$$

Or equivalent to

$$\begin{cases} \dot{x}_k = \frac{1}{2}\theta_k^*\boldsymbol{\varphi}_k^T(\widehat{\mathbf{x}}_k)\boldsymbol{\varphi}_k(\widehat{\mathbf{x}}_k) + g_k x_{k+1} + \phi_k \\ \dot{x}_n = \frac{1}{2}\theta_n^*\boldsymbol{\varphi}_n^T(\widehat{\mathbf{x}})\boldsymbol{\varphi}_n(\widehat{\mathbf{x}}) + g_n u + \phi_n \\ y = x_1 \end{cases}. \tag{17}$$

where $\phi_k = d_k + \Delta_k + c_k^*$, $k = 1, \ldots, n$ are lumped uncertainties at step k.

Assumption 3. [48]: With the investigated system (1), inequality (3), and transformations (15) and (17), there exist unknown positive boundaries D_k, $\overline{\Delta}_k$, and$\overline{C}_k$, $k = 1,\ldots, n$ such that $|\dot{d}_k| \le D_k, |\dot{\Delta}_k| \le \overline{\Delta}_k$, and$\left|\dot{c}_k^*\right| \le \overline{C}_k$, respectively.

Remark 4. The boundedness of the time derivative of d_k is a basic premise for extended state observer-based control [9,10,49]. $\dot{\Delta}_k$ is the function of system states which is physically bounded and is Lipschitz continuous, then, it is bounded, i.e.,$|\dot{\Delta}_k| \le \overline{\Delta}_k$. Similarly, without loss of generality, we have $c_k^* = \boldsymbol{\Xi}_k^{*T}\boldsymbol{\varphi}_k(\widehat{\mathbf{x}}_k) - \frac{1}{2}\theta_k^*\boldsymbol{\varphi}_k^T(\widehat{\mathbf{x}}_k)\boldsymbol{\varphi}_k(\widehat{\mathbf{x}}_k)$, and its absolute derivative is computed by $|\dot{c}_k^*| = |\frac{d}{dt}(\boldsymbol{\Xi}_k^{*T}\boldsymbol{\varphi}_k(\widehat{\mathbf{x}}_k)) - \frac{d}{dt}(\frac{1}{2}\theta_k^*\boldsymbol{\varphi}_k^T(\widehat{\mathbf{x}}_k)\boldsymbol{\varphi}_k(\widehat{\mathbf{x}}_k))|$ which is bounded because $\boldsymbol{\Xi}_k^*$ is an ideal weighting vector and it is definitely bounded while the Gaussian function $\boldsymbol{\varphi}_k(\widehat{\mathbf{x}}_k)$ is smooth and its derivative are constrained, then one can obtain $|\dot{c}_k^*| \le \overline{C}_k$. Therefore, Assumption 3 is reasonable. Even when the system is suddenly affected by external impacts such as disturbance or interaction or uncertainties, these impacts are not able to make an abrupt change and also need a certain time to influence the system's behavior. As a result, if $\phi_k = d_k + \Delta_k + c_k^*$ then the derivative of ϕ_k is bounded i.e., $\dot{\phi}_k = \dot{d}_k + \dot{\Delta}_k + \dot{c}_k^* \le |\dot{d}_k| + |\dot{\Delta}_k| + |\dot{c}_k^*| \le D_k + \overline{\Delta}_k + \overline{C}_k = \overline{\phi}_k$. However, the closed-loop stability cannot be guaranteed without appropriate controller and observer gains selections. Hence, this assumption is introduced to facilitate the control law design and stability proof.

Herein, the goal is to design a controller with adaptive laws for $\widehat{\theta}_k$ estimation and observers to estimate unmeasured state, x_k, and suppress mismatched lumped uncertainties ϕ_k. Due to unavailability of ideal θ_k^*, (17) cannot be used. Thus, instead of directly employing θ_k^* for the control law implementation, its estimation is utilized, i.e., $\frac{1}{2}\widehat{\theta}_k\boldsymbol{\varphi}_k^T(\widehat{\mathbf{x}}_k)\boldsymbol{\varphi}_k(\widehat{\mathbf{x}}_k)$, where $\widehat{\theta}_k = \|\,\widehat{\Xi}_k\|^2$ is an estimated norm of θ_k^*. For the sake of simplicity, hereafter, $\boldsymbol{\varphi}_k(\widehat{\mathbf{x}}_k)$ is shortened by $\boldsymbol{\varphi}_k$.

3.2. Nonlinear disturbance state observer

Conventionally, the Luenberger-like state observer was employed for unmeasured system states estimation. However, this cannot be effectively achieved in the case of (17) due to the impact of unknown ϕ_k. Regarding (17), one can realize that the performance of $\dot{x}_k$ depends on $x_{k+1}, f_k(\mathbf{x}_k)$, and d_k. Therefore, if employing an observer like $\dot{\widehat{x}}_k = \widehat{x}_{k+1} + l_k(y - \widehat{x}_1)$, one cannot obtain a true value of $\widehat{x}_{k+1}$ because the term $l_k(y - \widehat{x}_1)$ has no purpose of dealing with the unknown dynamics $f_k(\mathbf{x}_k)$ and d_k. It is just used to minimize the estimation error such that $\widehat{x}_k \to x_k$ by increasing an observer gain l_k. On the contrary, conventional disturbance observers such as [9–13] or other techniques required full or certain states measurement to tackle unknown disturbances and/or uncertainties, which brings a

barrier in this case when only an output is available. To overcome this obstacle, in this part, the NDSO for not only unmeasured states but also unknown lumped uncertainties estimation is established. The NDSO for the system states estimation and lumped disturbance rejection are described as

$$\begin{cases} \dot{\widehat{x}}_k = \frac{1}{2}\theta_k^* \boldsymbol{\varphi}_k^T \boldsymbol{\varphi}_k + g_k \widehat{x}_{k+1} + \frac{l_k(\delta)}{\sigma}(y - \widehat{x}_1) + \widehat{\phi}_k \\ \dot{\widehat{x}}_n = \frac{1}{2}\theta_n^* \boldsymbol{\varphi}_n^T \boldsymbol{\varphi}_n + g_n u + \frac{l_n(\delta)}{\sigma}(y - \widehat{x}_1) + \widehat{\phi}_n \end{cases} \quad y = x_1 \quad , \tag{18}$$

where $l_k(\delta)$ is a designed state observer gain at step k, σ is an arbitrarily scaled constant, δ is the bandwidth of the observer, and the terms $\widehat{\phi}_k$ are an estimation of the compound disturbance ϕ_k.

To obtain the estimated $\widehat{\phi}_k$, the following auxiliary variable is introduced:

$$\varepsilon_k = \phi_k - \omega_k x_k, \tag{19}$$

where $\omega_k > 0$ is a designed updating disturbance observer gain.

By taking derivative (19) with respect to time, the dynamics behavior of the auxiliary variable is expressed by:

$$\dot{\varepsilon}_k = \dot{\phi}_k - \omega_k \dot{x}_k = \dot{\phi}_k - \omega_k \left(\frac{1}{2}\theta_k^* \boldsymbol{\varphi}_k^T \boldsymbol{\varphi}_k + g_k \widehat{x}_{k+1} \right) - \omega_k(\varepsilon_k + \omega_k x_k). \tag{20}$$

Regarding [48], the adaptive law for mismatched disturbance estimation is derived with:

$$\begin{cases} \dot{\widehat{\varepsilon}}_k = -\omega_k \left(\frac{1}{2}\theta_k^* \boldsymbol{\varphi}_k^T \boldsymbol{\varphi}_k + g_k \widehat{x}_{k+1} + \widehat{\varepsilon}_k + \omega_k \widehat{x}_k \right), k = 1, \ldots, n-1 \\ \dot{\widehat{\varepsilon}}_n = -\omega_n \left(\frac{1}{2}\theta_n^* \boldsymbol{\varphi}_n^T \boldsymbol{\varphi}_n + g_n u + \widehat{\varepsilon}_n + \omega_n \widehat{x}_n \right) \end{cases} . \tag{21}$$

Subsequently, the estimation of the mismatched lumped disturbance can be expressed as

$$\widehat{\phi}_k = \widehat{\varepsilon}_k + \omega_k \widehat{x}_k \ (k = 1, 2, \ \ldots \ n). \tag{22}$$

Theorem 1. *Considered the rewritten model (18), adaptive laws (21) and (22) with suitable values l_k, ω_k and δ, unmeasured states x_k and lumped uncertainty ϕ_k can be observed and the estimated errors converge to the small neighbourhood of the origin in finite-time with the stability guaranteed.*

Proof. By subtracting (22) from (19), the lumped disturbance estimation error can be given as

$$\widetilde{\phi}_k = \widetilde{\varepsilon}_k + \omega_k \widetilde{x}_k. \tag{23}$$

Subtracting (21) from (20), one obtains the estimated error dynamics of mismatched uncertainties as

$$\begin{cases} \dot{\widetilde{\varepsilon}}_k = \dot{\varepsilon}_k - \dot{\widehat{\varepsilon}}_k = \dot{\phi}_k - \omega_k g_k \widetilde{x}_{k+1} - \omega_k(\widetilde{\varepsilon}_k + \omega_k \widetilde{x}_k), (k = 1, \ldots, n-1) \\ \dot{\widetilde{\varepsilon}}_n = \dot{\varepsilon}_n - \dot{\widehat{\varepsilon}}_n = \dot{\phi}_n - \omega_n(\widetilde{\varepsilon}_n + \omega_n \widetilde{x}_n) \end{cases} . \tag{24}$$

Moreover, by subtracting (18) from (17), the error dynamics of the state observer is obtained by:

$$\begin{cases} \dot{\mathbf{e}} = \frac{1}{\sigma}\mathbf{A}\mathbf{e} + \boldsymbol{\Phi} \\ \widetilde{y} = \widetilde{x}_1 \end{cases}, \tag{25}$$

where $\mathbf{e} = (x_1 - \widehat{x}_1 \quad x_2 - \widehat{x}_2 \quad \ldots \quad x_n - \widehat{x}_n)^T$, $\boldsymbol{\Phi} = (\widetilde{\phi}_1 \quad \widetilde{\phi}_2 \quad \ldots \quad \widetilde{\phi}_n)^T$, and $\mathbf{A} = \begin{bmatrix} -l_1(\delta) & \sigma g_1 & \ldots & 0 \\ -l_2(\delta) & 0 & \ddots & 0 \\ \vdots & \vdots & \ldots & \sigma g_{n-1} \\ -l_n(\delta) & 0 & \ldots & 0 \end{bmatrix}$.

Herein, the observer gains l_k should be designed such that the matrix $\mathbf{A}$ is Hurwitz. Thus, regarding the linear system theory, there exists a positive definite matrix $\mathbf{P}$ that satisfies:

$$\mathbf{A}^T\mathbf{P} + \mathbf{P}\mathbf{A} = -\mathbf{Q}. \tag{26}$$

Define a Lyapunov function W_0 as

$$W_0 = \frac{1}{2}\sum_{k=1}^{n} \widetilde{\varepsilon}_k^2 + \frac{1}{2}\mathbf{e}^T\mathbf{P}\mathbf{e}. \tag{27}$$

Then, by taking derivative W_0, one has:

$$\dot{W}_0 = \sum_{k=1}^{n} \widetilde{\varepsilon}_k \dot{\widetilde{\varepsilon}}_k + \frac{1}{2}\dot{\mathbf{e}}^T\mathbf{P}\mathbf{e} + \frac{1}{2}\mathbf{e}^T\mathbf{P}\dot{\mathbf{e}} = \sum_{k=1}^{n-1} \widetilde{\varepsilon}_k[\dot{\phi}_k - \omega_k g_k \widetilde{x}_{k+1} - \omega_k(\widetilde{\varepsilon}_k + \omega_k \widetilde{x}_k)] + \widetilde{\varepsilon}_n[\dot{\phi}_n - \omega_n(\widetilde{\varepsilon}_n + \omega_n \widetilde{x}_n)] - \frac{1}{2\sigma}\mathbf{e}^T\mathbf{Q}\mathbf{e} + \mathbf{e}^T\mathbf{P}\Phi$$
$$= -\sum_{k=1}^{n} \omega_k \widetilde{\varepsilon}_k^2 - \sum_{k=1}^{n} \omega_k^2 \widetilde{\varepsilon}_k \widetilde{x}_k + \sum_{k=1}^{n} \widetilde{\varepsilon}_k \dot{\phi}_k - \sum_{k=1}^{n-1} \omega_k \overline{g}_k \widetilde{\varepsilon}_k \widetilde{x}_{k+1} - \frac{1}{2\sigma}\mathbf{e}^T\mathbf{Q}\mathbf{e} + \mathbf{e}^T\mathbf{P}\Phi \quad (28)$$

Applying Young's inequality for each term in (28) yields:

$$-\sum_{k=1}^{n} \omega_k^2 \widetilde{\varepsilon}_k \widetilde{x}_k \le \frac{1}{2}\sum_{k=1}^{n} \widetilde{\varepsilon}_k^2 + \frac{1}{2}\overline{\omega}^4 \mathbf{e}^T\mathbf{e}. \quad (29)$$

$$\sum_{k=1}^{n} \widetilde{\varepsilon}_k \dot{\phi}_k \le \frac{1}{2}\sum_{k=1}^{n} \widetilde{\varepsilon}_k^2 + \frac{1}{2}\sum_{k=1}^{n} \overline{\phi}_k^2. \quad (30)$$

$$-\sum_{k=1}^{n-1} \omega_k \overline{g}_k \widetilde{\varepsilon}_k \widetilde{x}_{k+1} \le \frac{1}{2}\sum_{k=1}^{n} \widetilde{\varepsilon}_k^2 + \frac{1}{2}\overline{\omega}^2 \overline{g}^2 \mathbf{e}^T\mathbf{e}. \quad (31)$$

$$\mathbf{e}^T\mathbf{P}\Phi \le \frac{1}{2}\mathbf{e}^T \| \mathbf{P} \|^2 \mathbf{e} + \frac{1}{2}\sum_{k=1}^{n} \widetilde{\phi}_k^2 = \frac{1}{2}\mathbf{e}^T \| \mathbf{P} \|^2 \mathbf{e} + \frac{1}{2}\sum_{k=1}^{n} (\widetilde{\varepsilon}_k + \omega_k \widetilde{x}_k)^2 \le \frac{1}{2}\mathbf{e}^T \| \mathbf{P} \|^2 \mathbf{e} + \sum_{k=1}^{n} \widetilde{\varepsilon}_k^2 + \overline{\omega}^2 \mathbf{e}^T\mathbf{e}. \quad (32)$$

where $\overline{\phi}_k$ is an upper bound of $\dot{\phi}_k$, i.e., $|\dot{\phi}_k| \le \overline{\phi}_k$ obtained as a result from *Assumption 3*, $\overline{\omega} = \max(\omega_k), \overline{g} = \max(g_k)$, $\|\mathbf{P}\|^2$ is an Euclidean norm of matrix **P**.

Considering (29) to (32), one has:

$$\dot{W}_0 \le -\frac{1}{2}\mathbf{e}^T\left(\frac{1}{\sigma}\lambda\min(\mathbf{Q}) - \| \mathbf{P} \|^2 - \overline{\omega}^2(1+\overline{g}^2) - \overline{\omega}^4\right)\mathbf{e} - \frac{1}{2}\sum_{k=1}^{n}(2\omega_k - 5)\widetilde{\varepsilon}_k^2 + \frac{1}{2}\sum_{k=1}^{n}\overline{\phi}_k^2. \quad (33)$$

Moreover, by extending (33) with *Lemma 1*, the following inequalities are obtained:

$$(\mathbf{e}^T\mathbf{P}\mathbf{e})^{\frac{\iota+1}{2}} \le \frac{\left[(\mathbf{e}^T\mathbf{P}\mathbf{e})^{\iota+1/2}\right]^{\frac{2}{\iota+1}}}{\frac{2}{\iota+1}} + \frac{1^{\frac{2}{1-\iota}}}{\frac{2}{1-\iota}} = \frac{\iota+1}{2}(\mathbf{e}^T\mathbf{P}\mathbf{e}) + \frac{1-\iota}{2}, \quad (34)$$

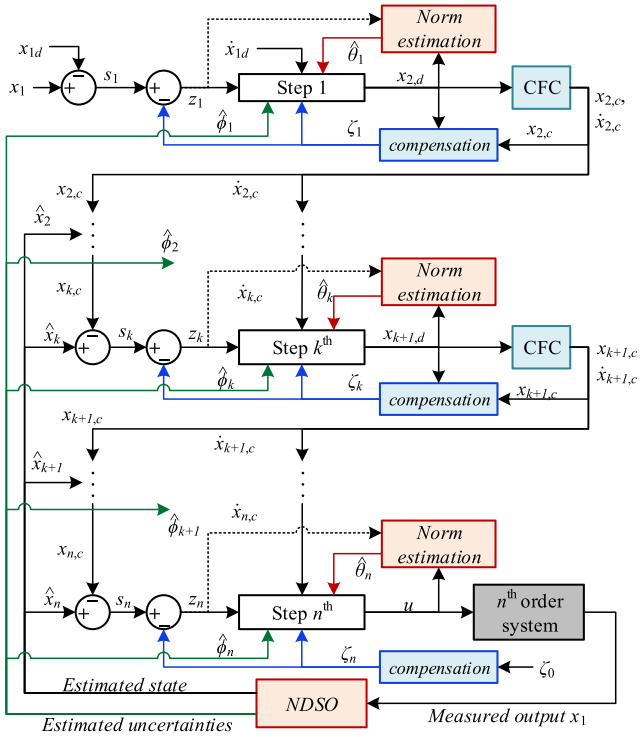

Fig. 1. Structure of the proposed control scheme with state observer and CF with compensator mechanisms.

$$\sum_{k=1}^{n}\left(\widetilde{\varepsilon}_k^2\right)^{\frac{\iota+1}{2}} \le \frac{\sum_{k=1}^{n}\left[\left(\widetilde{\varepsilon}_k^2\right)^{\iota+1|2}\right]^{\frac{2}{\iota+1}}}{\frac{2}{\iota+1}} + n\frac{1^{\frac{2}{1-\iota}}}{\frac{2}{1-\iota}} = \frac{\iota+1}{2}\sum_{k=1}^{n}\widetilde{\varepsilon}_k^2 + \frac{n(1-\iota)}{2}, \tag{35}$$

where $0 < \iota < 1$ and $\iota = p/q$ with p, q being odd constants that satisfy $2p/q > 1$.

Consequently, W_0 is constrained by:

$$\begin{aligned}\dot{W}_0 \le\ & -\frac{1}{2}\mathbf{e}^T\left(\frac{1}{\sigma}\lambda_{\min}(\mathbf{Q}) - \| \mathbf{P} \|^2 - (\iota+1)\| \mathbf{P} \|^2 - \overline{\omega}^2\left(1+\overline{g}^2\right) - \overline{\omega}^4\right)\mathbf{e} - \frac{1}{2}\sum_{k=1}^{n}(2\omega_k - 6 - \iota)\widetilde{\varepsilon}_k^2 - \left(\mathbf{e}^T\mathbf{P}\mathbf{e}\right)^{\frac{\iota+1}{2}} - \sum_{k=1}^{n}\left(\widetilde{\varepsilon}_k^2\right)^{\frac{\iota+1}{2}} \\ & + \frac{1}{2}\sum_{k=1}^{n}\overline{\phi}_k^2 + \frac{(n+1)(1-\iota)}{2}\end{aligned} \tag{36}$$

Regarding (36), values of ω_k and σ can be designed to guarantee the stability of the NDSO. However, as the coupling dynamics of the lumped disturbances ϕ_k, state estimation x_k, and unknown terms $\boldsymbol{\Xi}_k^{*T}\boldsymbol{\varphi}_k(\mathbf{x})$, to achieve the closed-loop system stability, the control law and values of ω_k and σ should be appropriately designed such that all approximation and estimated errors are bounded and converge to the neighbourhood of the origin in finite-time.

4. Proposed control scheme

4.1. Control laws implementation

In this section, a proposed observer-based BSC-RBFNN is conducted for non-strict feedback nonlinear system to satisfy tracking regulation. The proposed control scheme is sketched out in Fig. 1.

For tracking regulation, let's define the tracking errors.

$$\begin{cases} s_1 = x_1 - x_{1,\mathrm{d}} \\ s_k = \widehat{x}_k - x_{k,\mathrm{c}},\ k = 2, \ldots, n\,. \\ z_i = s_i - \zeta_i,\ i = 1, \ldots, n \end{cases} \tag{37}$$

where s_k are the system states tracking errors,$\widehat{x}_k$and $x_{k,c}$ are, in turn, the estimated states and filtered intermediate virtual control signals; z_k are auxiliary compensated tracking errors; and ζ_k are the compensation errors that satisfy:

$$\begin{cases} \dot{\zeta}_1 = -\kappa_1\zeta_1 + g_1\left(\widehat{x}_{2,c} - x_{2,d}\right) + g_1\zeta_2 \\ \dot{\zeta}_k = -\kappa_k\zeta_k + g_k\left(x_{k+1,c} - x_{k+1,d}\right) - g_{k-1}\zeta_{k-1} + g_k\zeta_{k+1};\ (k = 2, \ldots, n-1) \\ \dot{\zeta}_n = -\kappa_n\zeta_n - g_{n-1}\zeta_{n-1} \\ \zeta(0) = 0 \end{cases}. \tag{38}$$

Step 1: Define a Lyapunov candidate W_1 as

$$W_1 = W_0 + \frac{1}{2}z_1^2 + \frac{1}{2\gamma_1}\widetilde{\theta}_1^2 + \frac{1}{2}\zeta_1^2. \tag{39}$$

where $\widetilde{\theta}_1 = \theta_1^* - \widehat{\theta}_1$ and $\dot{\widetilde{\theta}}_1 = -\dot{\widehat{\theta}}_1$.

Taking derivative W_1 results in:

$$\dot{W}_1 = \dot{W}_0 + z_1\left(\dot{x}_1 - \dot{x}_{1,d} - \dot{\zeta}_1\right) - \frac{1}{\gamma_1}\widetilde{\theta}_1\dot{\widehat{\theta}}_1 + \zeta_1\dot{\zeta}_1. \tag{40}$$

From (17), (40) is expressed as

$$\begin{aligned}\dot{W}_1 = \dot{W}_0 + z_1\Bigg(\frac{1}{2}\widehat{\theta}_1\boldsymbol{\varphi}_1^T\boldsymbol{\varphi}_1 + \frac{l_1(\delta)}{\sigma}(y - \widehat{x}_1) - \dot{x}_{1,d} + g_1x_{2,d} + \phi_1 + g_1s_2 + g_1\left(x_{2,c} - x_{2,d}\right) - \dot{\zeta}_1\Bigg) \\ + \frac{1}{2}z_1\widetilde{\theta}_1\boldsymbol{\varphi}_1^T\boldsymbol{\varphi}_1 - \frac{1}{\gamma_1}\widetilde{\theta}_1\dot{\widehat{\theta}}_1 + \zeta_1\dot{\zeta}_1.\end{aligned} \tag{41}$$

To guarantee the stability of (41), the intermediate virtual control and adaptive law are adopted as

$$\begin{cases} x_{2,d} = \dfrac{1}{g_1}\left(-\dfrac{1}{2}\widehat{\theta}_1\boldsymbol{\varphi}_1^T\boldsymbol{\varphi}_1 + \dot{x}_{1,d} - \widehat{\phi}_1 - \dfrac{l_1(\delta)}{\sigma}(y-\widehat{x}_1) - \kappa_1 s_1 - \eta_1 z_1^{\iota} \right) \\ \dot{\widehat{\theta}}_1 \end{cases} = \frac{1}{2}\gamma_1 z_1 \boldsymbol{\varphi}_1^T\boldsymbol{\varphi}_1 - \lambda_1\widehat{\theta}_1. \tag{42}$$

where κ_1 and η_1 are controller gains, and $\kappa_1 > 1$; γ_1 and λ_1 denote arbitrarily constants to update the estimated norm $\widehat{\theta}_1$.

Substituting control laws (42) into (41) results in:

$$\dot{W}_1 = \dot{W}_0 - \kappa_1 z_1^2 - \eta_1 z_1^{\iota+1} + g_1 z_1 z_2 + \frac{\lambda_1}{\gamma_1}\widetilde{\theta}_1\widehat{\theta}_1 + \zeta_1\dot{\zeta}_1 + z_1\widetilde{\phi}_1. \tag{43}$$

It is obvious that the following inequalities are satisfied:

$$\begin{cases} \dfrac{\lambda_1}{\gamma_1}\widetilde{\theta}_1\widehat{\theta}_1 = \dfrac{\lambda_1}{\gamma_1}\widetilde{\theta}_1\left(\theta_1^* - \widetilde{\theta}_1\right) \le -\dfrac{\lambda_1}{2\gamma_1}\widetilde{\theta}_1^2 + \dfrac{\lambda_1}{2\gamma_1}\theta_1^{*2} \\ z_1\widetilde{\phi}_1 = z_1(\widetilde{\varepsilon}_1 + \omega_1\widetilde{x}_1) \le z_1^2 + \dfrac{1}{2}\widetilde{\varepsilon}_1^2 + \dfrac{1}{2}\omega_1^2\widetilde{x}_1^2 \end{cases}. \tag{44}$$

Subsequently, the derivative of W_1 is constrained by:

$$\dot{W}_1 \le \dot{W}_0 - (\kappa_1 - 1)z_1^2 - \eta_1\left(z_1^2\right)^{\frac{\iota+1}{2}} - \frac{\lambda_1}{2\gamma_1}\widetilde{\theta}_1^2 + \frac{1}{2}\widetilde{\varepsilon}_1^2 + \frac{1}{2}\omega_1^2\widetilde{x}_1^2 + g_1 z_1 z_2 + \frac{\lambda_1}{2\gamma_1}\theta_1^{*2} + \zeta_1\dot{\zeta}_1. \tag{45}$$

Step *k* (k=2, …, n–1): Define a Lyapunov candidate W_k as

$$W_k = W_{k-1} + \frac{1}{2}z_k^2 + \frac{1}{2\gamma_k}\widetilde{\theta}_k^2 + \frac{1}{2}\zeta_k^2. \tag{46}$$

where $\widetilde{\theta}_k = \theta_k^* - \widehat{\theta}_k$ and$\dot{\widetilde{\theta}}_k = -\dot{\widehat{\theta}}_k$.

Similarly, by taking the derivative W_k with respect to time, one obtains:

$$\dot{W}_k = \dot{W}_{k-1} + z_k\left(\dot{\widehat{x}}_k - \dot{x}_{k,c} - \dot{\zeta}_k\right) - \frac{1}{\gamma_k}\widetilde{\theta}_k\dot{\widehat{\theta}}_k + \zeta_k\dot{\zeta}_k. \tag{47}$$

Expressing the *k* sub-system yields:

$$\begin{aligned} \dot{W}_k = \dot{W}_{k-1} + z_k\left(\frac{1}{2}\theta_k^*\varphi_k^T\varphi_k + g_k\widehat{x}_{k+1}\frac{l_k(\delta)}{\sigma}(y-\widehat{x}_1) - \dot{x}_{k,c} + \phi_k - \dot{\zeta}_k\right) - \frac{1}{\gamma_k}\widetilde{\theta}_k\dot{\widehat{\theta}}_k + \zeta_k\dot{\zeta}_k \qquad = \dot{W}_{k-1} \\ + z_k\left(\frac{1}{2}\widehat{\theta}_k\varphi_k^T\varphi_k - g_k x_{k+1,d} + \frac{l_k(\delta)}{\sigma}(y-\widehat{x}_1) - \dot{x}_{k,c} + \phi_k + g_k s_{k+1} + g_k\left(x_{k+1,c} - x_{k+1,d}\right)_k - \dot{\zeta}_k\right) + \frac{1}{2}z_k\widetilde{\theta}_k\varphi_k^T\varphi_k - \frac{1}{\gamma_k}\widetilde{\theta}_k\dot{\widehat{\theta}}_k + \zeta_k\dot{\zeta}_k \end{aligned}. \tag{48}$$

Then, the intermediate virtual control signal and adaptive law for norm estimation are adopted as

$$\begin{cases} x_{k+1,d} = \dfrac{1}{g_k}\left(-\dfrac{1}{2}\widehat{\theta}_k\boldsymbol{\varphi}_k^T\boldsymbol{\varphi}_k + \dot{x}_{k,c} - \dfrac{l_k(\delta)}{\sigma}(y-\widehat{x}_1) - \widehat{\phi}_k - \kappa_k s_k - \eta_k z_k^{\iota} - g_{k-1}s_{k-1} \right) \\ \dot{\widehat{\theta}}_k \end{cases} = \frac{1}{2}\gamma_k z_k\boldsymbol{\varphi}_k^T\boldsymbol{\varphi}_k - \lambda_k\widehat{\theta}_k, \tag{49}$$

where κ_k and η_k are controller gains and $\kappa_k > 1$; γ_k and λ_k denote arbitrarily constants to update the estimated norm $\widehat{\theta}_k$.

Substituting control laws (49) into (48) results in:

$$\dot{W}_k = \dot{W}_{k-1} - \kappa_k z_k^2 - \eta_k z_k^{\iota+1} - g_{k-1}z_{k-1}z_k + g_k z_k z_{k+1} + \frac{\lambda_k}{\gamma_k}\widetilde{\theta}_k\widehat{\theta}_k + z_k\widetilde{\phi}_k + \zeta_k\dot{\zeta}_k. \tag{50}$$

It is obvious that the following inequalities are satisfied:

$$\begin{cases} \dfrac{\lambda_k}{\gamma_k}\widetilde{\theta}_k\widehat{\theta}_k = \dfrac{\lambda_k}{\gamma_k}\widetilde{\theta}_k\left(\theta_k^* - \widetilde{\theta}_k\right) \le -\dfrac{\lambda_k}{2\gamma_k}\widetilde{\theta}_k^2 + \dfrac{\lambda_k}{2\gamma_k}\theta_k^{*2} \\ z_k\widetilde{\phi}_k = z_k(\widetilde{\varepsilon}_k + \omega_k\widetilde{x}_k) \le z_k^2 + \dfrac{1}{2}\widetilde{\varepsilon}_k^2 + \dfrac{1}{2}\omega_k^2\widetilde{x}_k^2 \end{cases}. \tag{51}$$

Subsequently, the derivative of W_k is constrained by:

$$\dot{W}_k \le \dot{W}_{k-1} - (\kappa_k - 1)z_k^2 - \eta_k\left(z_k^2\right)^{\frac{\iota+1}{2}} - \frac{\lambda_k}{2\gamma_k}\widetilde{\theta}_k^2 - g_{k-1}z_{k-1}z_k + g_k z_k z_{k+1} + \frac{\lambda_k}{2\gamma_k}\theta_k^{*2} + \frac{1}{2}\widetilde{\varepsilon}_k^2 + \frac{1}{2}\omega_k^2\widetilde{x}_k^2 + \zeta_k\dot{\zeta}_k. \tag{52}$$

It is noteworthy that, by following control laws (49), the term existing from the previous step is cancelled out in this step, and the term $g_k z_k z_{k+1}$ raising in this step will subsequently be cancelled in the next step.

By expressing the derivative of W_{k-1}, (52) becomes:

$$\dot{W}_k \le \dot{W}_0 - \sum_{i=1}^{k}(\kappa_i - 1)z_i^2 - \sum_{i=1}^{k}\eta_i z_i^{\iota+1} - \sum_{i=1}^{k}\frac{\lambda_i}{2\gamma_i}\widetilde{\theta}_i^2 + g_k z_k z_{k+1} + \frac{1}{2}\sum_{i=1}^{k}\widetilde{\varepsilon}_i^2 + \frac{1}{2}\sum_{i=1}^{k}\omega_i^2\widetilde{x}_i^2 + \sum_{i=1}^{k}\frac{\lambda_i}{2\gamma_i}\theta_i^{*2} + \sum_{i=1}^{k}\zeta_i\dot{\zeta}_i. \tag{53}$$

Step *n*: Define a Lyapunov candidate W_n as

$$W_n = W_{n-1} + \frac{1}{2}z_n^2 + \frac{1}{2\gamma_n}\widetilde{\theta}_n^2 + \frac{1}{2}\zeta_n^2. \tag{54}$$

where $\widetilde{\theta}_n = \theta_n^* - \widehat{\theta}_n$ and $\dot{\widetilde{\theta}}_n = -\dot{\widehat{\theta}}_n$.

Taking derivative W_n, with respect to time, results in:

$$\dot{W}_n = \dot{W}_{n-1} + z_n\left(\dot{\widehat{x}}_n - \dot{x}_{n,c} - \dot{\zeta}_n\right) - \frac{1}{\gamma_n}\widetilde{\theta}_n\dot{\widehat{\theta}}_n + \zeta_n\dot{\zeta}_n. \tag{55}$$

Expressing sub-system n yields:

$$\begin{aligned}\dot{W}_n = \dot{W}_{n-1} + z_k\Bigg(&\frac{1}{2}\widehat{\theta}_n\boldsymbol{\varphi}_n^T\boldsymbol{\varphi}_n + g_n u + \frac{l_n(\delta)}{\sigma}(y - \widehat{x}_1) - \dot{x}_{n,c} + \boldsymbol{\phi}_n + g_k s_{k+1} + g_k\left(x_{k+1,c} - x_{k+1,d}\right)_k - \dot{\zeta}_k\Bigg) \\ &+\frac{1}{2}z_n\widetilde{\theta}_k\boldsymbol{\varphi}_n^T\boldsymbol{\varphi}_n - \frac{1}{\gamma_n}\widetilde{\theta}_n\dot{\widehat{\theta}}_n\end{aligned} + \zeta_n\dot{\zeta}_n. \tag{56}$$

Hence, the control input signal and adaptive law for norm estimation are adopted as

$$\begin{cases} u = \dfrac{1}{g_n}\left(-\dfrac{1}{2}\widehat{\theta}_n\boldsymbol{\varphi}_n^T\boldsymbol{\varphi}_n - \dfrac{l_n(\delta)}{\sigma}(y - \widehat{x}_1) + \dot{x}_{n,c} - \widehat{\phi}_n - \kappa_n s_n - \eta_n z_n^{\iota} - g_{n-1}s_{n-1}\right) \\ \dot{\widehat{\theta}}_n = \dfrac{1}{2}\gamma_n z_n\boldsymbol{\varphi}_n^T\boldsymbol{\varphi}_n - \lambda_n\widehat{\theta}_n. \end{cases} \tag{57}$$

where κ_n and η_n are controller gains, and $\kappa_n > 1$; γ_n and λ_n denote arbitrarily constants to update the estimated norm $\widehat{\theta}_n$.

Substituting control laws (57) into (56) results in:

$$\begin{aligned}\dot{W}_n &= \dot{W}_{n-1} + z_n\left(-\kappa_n s_n - \eta_n z_n^{\iota} - g_{n-1}s_{n-1} - \dot{\zeta}_k\right) + \frac{1}{\gamma_n}\lambda_n\widetilde{\theta}_n\widehat{\theta}_n + z_n\widetilde{\phi}_n + \zeta_n\dot{\zeta}_n \\ &= \dot{W}_{n-1} - \kappa_n z_n^2 - \eta_n z_n^{\iota} - g_{n-1}z_{n-1}z_n + \frac{1}{\gamma_n}\lambda_n\widetilde{\theta}_n\widehat{\theta}_n + z_n\widetilde{\phi}_n + \zeta_n\dot{\zeta}_n\end{aligned}. \tag{58}$$

Similarly, the following inequalities are satisfied:

$$\begin{cases} \dfrac{\lambda_n}{\gamma_n}\widetilde{\theta}_n\widehat{\theta}_n \le -\dfrac{\lambda_n}{2\gamma_n}\widetilde{\theta}_n^2 + \dfrac{\lambda_n}{2\gamma_n}\theta_n^{*2} \\ z_n\widetilde{\phi}_n = z_n(\widetilde{\varepsilon} + \omega_n\widetilde{x}_n) \le z_n^2 + \dfrac{1}{2}\widetilde{\varepsilon}_n^2 + \dfrac{1}{2}\omega_n^2\widetilde{x}_n^2 \end{cases}. \tag{59}$$

Subsequently, the derivative of W_n is constrained by:

$$\dot{W}_n \le \dot{W}_{n-1} - (\kappa_n - 1)z_n^2 - \eta_n z_n^{\iota+1} - \frac{\lambda_n}{2\gamma_n}\widetilde{\theta}_n^2 - g_{n-1}z_{n-1}z_n + \frac{\lambda_n}{2\gamma_n}\theta_n^{*2} + \frac{1}{2}\widetilde{\varepsilon}_n^2 + \frac{1}{2}\omega_n^2\widetilde{x}_n^2 + \zeta_n\dot{\zeta}_n. \tag{60}$$

By expressing the derivative of W_{n-1}, (61) becomes:

$$\begin{aligned}\dot{W}_n &\le \dot{W}_0 - \sum_{k=1}^{n}(\kappa_k-1)z_i^2 - \sum_{k=1}^{n}\eta_k\left(z_k^2\right)^{\frac{\iota+1}{2}} - \sum_{k=1}^{n}\frac{\lambda_k}{2\gamma_k}\widetilde{\theta}_k^2 + \frac{1}{2}\sum_{k=1}^{n}\widetilde{\varepsilon}_k^2 + \frac{1}{2}\sum_{k=1}^{n}\omega_k^2\widetilde{x}_k^2 + \sum_{k=1}^{n}\frac{\lambda_k}{2\gamma_k}\theta_i^{*2} + \sum_{k=1}^{n}\zeta_k\dot{\zeta}_k \\ &\le -\frac{1}{2}\mathbf{e}^T\left(\frac{\lambda_{\min}(\mathbf{Q})}{\sigma} - \|\mathbf{P}\|^2 - (\iota+1)\mathbf{P} - \left(\overline{\omega}^2\left(1+\overline{g}^2\right)+\overline{\omega}^4\right)\mathbf{I}_n\right)\mathbf{e} - \frac{1}{2}\sum_{k=1}^{n}(2\omega_k - 7 - \iota)\widetilde{\varepsilon}_k^2 \\ &\quad -\left(\mathbf{e}^T\mathbf{P}\mathbf{e}\right)^{\frac{\iota+1}{2}} - \sum_{k=1}^{n}\left(\widetilde{\varepsilon}_k^2\right)^{\frac{\iota+1}{2}} - \sum_{k=1}^{n}(\kappa_k-1)z_k^2 - \sum_{k=1}^{n}\eta_k\left(z_k^2\right)^{\frac{\iota+1}{2}} - \sum_{k=1}^{n}\frac{\lambda_k}{2\gamma_k}\widetilde{\theta}_k^2 + \frac{1}{2}\sum_{k=1}^{n}\widetilde{\varepsilon}_k^2 \\ &\quad +\frac{1}{2}\sum_{k=1}^{n}\omega_k^2\widetilde{x}_k^2 + \sum_{k=1}^{n}\frac{\lambda_k}{2\gamma_k}\theta_k^{*2} + \frac{1}{2}\sum_{k=1}^{n}\overline{\phi}_k^2 + \frac{(n+1)(1-\iota)}{2} + \sum_{k=1}^{n}\zeta_k\dot{\zeta}_k\end{aligned} \tag{61}$$

In view of *Lemma 4*, the error compensation term, $\sum_{i=1}^{n}\zeta_i\dot{\zeta}_i$, is constrained by:

$$\sum_{i=1}^{n}\zeta_i\dot{\zeta}_i = -\sum_{i=1}^{n}\kappa_i\zeta_i^2 + \sum_{i=1}^{n-1}g_i\left(x_{i+1,c} - x_{i+1,d}\right) \le -\sum_{i=1}^{n}\kappa_i\zeta_i^2 + \sum_{i=1}^{n-1}g_i\varpi_{i+1}. \tag{62}$$

Then, one has:

$$\begin{aligned}\dot{W}_n &\le -\frac{1}{2}\mathbf{e}^T\left(\frac{\lambda_{\min}(\mathbf{Q})}{\sigma} - \|\mathbf{P}\|^2 - (\iota+1)\|\mathbf{P}\|^2 - \left(\overline{\omega}^2\left(2+\overline{g}^2\right)+\overline{\omega}^4\right)\right)\mathbf{e} - \frac{1}{2}\sum_{k=1}^{n}(2\omega_k - 7 - \iota)\widetilde{\varepsilon}_k^2 \\ &\quad -\left(\mathbf{e}^T\mathbf{P}\mathbf{e}\right)^{\frac{\iota+1}{2}} - \sum_{k=1}^{n}\left(\widetilde{\varepsilon}_k^2\right)^{\frac{\iota+1}{2}} - \sum_{k=1}^{n}(\kappa_k-1)z_i^2 - \sum_{k=1}^{n}\eta_k\left(z_k^2\right)^{\frac{\iota+1}{2}} - \sum_{k=1}^{n}\frac{\lambda_k}{2\gamma_k}\widetilde{\theta}_k^2 \\ &\quad +\sum_{k=1}^{n}\frac{\lambda_k}{2\gamma_k}\theta_k^{*2} + \frac{1}{2}\sum_{k=1}^{n}\overline{\phi}_k^2 + \frac{(n+1)(1-\iota)}{2} - \sum_{k=1}^{n}\kappa_k\zeta_k^2 + \sum_{k=1}^{n-1}g_k\varpi_{k+1}\end{aligned} \tag{63}$$

4.2. Closed-loop system stability proof

Theorem 2. *Consider system (1) with Assumptions 1, 2, and 3, Lemmas 1, 2, 3, and 4, NDSO (21), system transformations (17), DSC adopted (8), error compensation (38), along with control laws, and norm estimations at each step in (42), (49), and (57) the closed-loop system is guaranteed to be SGPFS and converge to the small neighbourhood of the origin in finite-time.*

Proof. The result (63) is modified as

$$\begin{aligned}\dot{W}_n &\le -\frac{1}{2}\mathbf{e}^T\left(\frac{\lambda_{\min}(\mathbf{Q})}{\sigma} - \|\mathbf{P}\|^2 - (\iota+1)\|\mathbf{P}\|^2 - \left(\overline{\omega}^2\left(2+\overline{g}^2\right)+\overline{\omega}^4\right)\right)\mathbf{e} - \frac{1}{2}\sum_{k=1}^{n}(2\omega_k - 7 - \iota)\widetilde{\varepsilon}_k^2 \\ &\quad -\left(\mathbf{e}^T\mathbf{P}\mathbf{e}\right)^{\frac{\iota+1}{2}} - \sum_{k=1}^{n}\left(\widetilde{\varepsilon}_k^2\right)^{\frac{\iota+1}{2}} - \sum_{k=1}^{n}(\kappa_k-1)z_k^2 - \sum_{k=1}^{n}\eta_k\left(z_k^2\right)^{\frac{\iota+1}{2}} - \sum_{k=1}^{n}\frac{\lambda_k}{2\gamma_k}\widetilde{\theta}_k^2 \\ &\quad -\sum_{k=1}^{n}\frac{\lambda_k}{2\gamma_k}\left(\widetilde{\theta}_k^2\right)^{\frac{\iota+1}{2}} + \sum_{k=1}^{n}\frac{\lambda_k}{2\gamma_k}\left(\widetilde{\theta}_k^2\right)^{\frac{\iota+1}{2}} - \sum_{k=1}^{n}\left(\zeta_k^2\right)^{\frac{\iota+1}{2}} + \sum_{k=1}^{n}\left(\zeta_k^2\right)^{\frac{\iota+1}{2}} \\ &\quad +\sum_{k=1}^{n}\frac{\lambda_k}{2\gamma_k}\theta_k^{*2} + \frac{1}{2}\sum_{k=1}^{n}\overline{\phi}_k^2 + \frac{(n+1)(1-\iota)}{2} - \sum_{k=1}^{n}\kappa_k\zeta_k^2 + \sum_{k=1}^{n-1}g_k\varpi_{k+1}\end{aligned} \tag{64}$$

By applying *Lemma 1*, one obtains:

$$\sum_{k=1}^{n}\frac{\lambda_k}{2\gamma_k}\left(\widetilde{\theta}_k^2\right)^{\frac{\iota+1}{2}} \le \sum_{k=1}^{n}\frac{\lambda_k}{2\gamma_k}\frac{\left[\left(\widetilde{\theta}_k^2\right)^{\frac{\iota+1}{2}}\right]^{\frac{2}{\iota+1}}}{\frac{2}{\iota+1}} + \sum_{k=1}^{n}\frac{\lambda_k}{2\gamma_k}\frac{1^{\frac{2}{1-\iota}}}{\frac{2}{1-\iota}} = \frac{1}{2}\sum_{k=1}^{n}\frac{\lambda_k}{2\gamma_k}(\iota+1)\widetilde{\theta}_k^2 + \sum_{k=1}^{n}\frac{\lambda_k(1-\iota)}{4\gamma_k}. \tag{65}$$

$$\sum_{k=1}^{n}\left(\zeta_k^2\right)^{\frac{\iota+1}{2}} \le \frac{1}{2}\sum_{k=1}^{n}(\iota+1)\zeta_k^2 + \frac{n(1-\iota)}{2}. \tag{66}$$

From (66) and (65), inequality (64) is rewritten as

$$\begin{aligned}\dot{W}_n \le & -\frac{1}{2}\mathbf{e}^T\left(\frac{\lambda_{\min}(\mathbf{Q})}{\sigma} - \| \mathbf{P} \|^2 - (\iota+1)\| \mathbf{P} \|^2 - \left(\overline{\omega}^2\left(2+\overline{g}^2\right)+\overline{\omega}^4\right)\right)\mathbf{e} - \frac{1}{2}\sum_{k=1}^{n}(2\omega_k - 7 - \iota)\widetilde{\varepsilon}_k^2 \\ & -\left(\mathbf{e}^T\mathbf{P}\mathbf{e}\right)^{\frac{\iota+1}{2}} - \sum_{k=1}^{n}\left(\widetilde{\varepsilon}_k^2\right)^{\frac{\iota+1}{2}} - \sum_{k=1}^{n}(\kappa_k - 1)z_k^2 - \sum_{i=1}^{n}\frac{1}{4\gamma_k}\lambda_k(1-\iota)\widetilde{\theta}_i^2 - \frac{1}{2}\sum_{k=1}^{n}(2\kappa_k - 1 - \iota)\zeta_k^2 \\ & -\sum_{k=1}^{n}\eta_k\left(z_k^2\right)^{\frac{\iota+1}{2}} - \sum_{i=1}^{n}\frac{\lambda_k}{2\gamma_k}\left(\widetilde{\theta}_k^2\right)^{\frac{\iota+1}{2}} - \sum_{k=1}^{n}\left(\zeta_k^2\right)^{\frac{\iota+1}{2}} + \sum_{k=1}^{n}\frac{\lambda_k}{2\gamma_k}\theta_k^{*2} \\ & +\frac{1}{2}\sum_{k=1}^{n}\overline{\phi}_k^2 + \frac{(n+1)(1-\iota)}{2} + \sum_{k=1}^{n-1}g_k\varpi_{k+1} + \sum_{k=1}^{n}\frac{\lambda_k(1-\iota)}{4\gamma_k} + \frac{n(1-\iota)}{2}\end{aligned} \tag{67}$$

From (67), it is obvious that to guarantee the stability of the closed-loop system, the values of positive parameters σ, ω_k, κ_k should be adopted such that they satisfy: $\kappa_k > 1$, $\frac{1}{\sigma}\lambda_{\min}(\mathbf{Q}) - \| \mathbf{P} \|^2 - (\iota+1)\| \mathbf{P} \|^2 - (\overline{\omega}^2(2+\overline{g}^2)+\overline{\omega}^4) > 0$, and $2\omega_k - 7 - \iota > 0$.

In view of *Lemma 2*, one has:

$$\begin{aligned}&\left(\mathbf{e}^T\mathbf{P}\mathbf{e}\right)^{\frac{\iota+1}{2}} + \sum_{k=1}^{n}\left(\widetilde{\varepsilon}_k^2\right)^{\frac{\iota+1}{2}} + \sum_{i=1}^{n}\eta_i\left(z_i^2\right)^{\frac{\iota+1}{2}} + \sum_{i=1}^{n}\frac{\lambda_i}{2\gamma_i}\left(\widetilde{\theta}_i^2\right)^{\frac{\iota+1}{2}} + \sum_{i=1}^{n}\left(\zeta_i^2\right)^{\frac{\iota+1}{2}} \\ &\ge \Gamma_2\left(\frac{1}{2}\left(\mathbf{e}^T\mathbf{P}\mathbf{e}\right) + \sum_{i=1}^{n}\frac{1}{2}\widetilde{\varepsilon}_k^2 + \sum_{i=1}^{n}\frac{1}{2}z_i^2 + \sum_{i=1}^{n}\frac{1}{2\gamma_i}\widetilde{\theta}_i^2 + \sum_{i=1}^{n}\frac{1}{2}\zeta_i^2\right)^{\frac{\iota+1}{2}}\end{aligned} \tag{68}$$

As a result, the derivative of W_n is bounded by:

$$\dot{W}_n \le -\Gamma_1 W_n - \Gamma_2 W_n^{\frac{\iota+1}{2}} + C\,. \tag{69}$$

with $\Gamma_1 = \min\left\{\frac{\lambda_{\min}(\mathbf{Q})}{\sigma} - \| \mathbf{P} \|^2 - (\iota+1)\| \mathbf{P} \|^2 - (\overline{\omega}^2(2+\overline{g}^2)+\overline{\omega}^4), (2\omega_k - 7 - \iota), 2(\kappa_k - 1), \lambda_k(1-\iota), (2\kappa_k - 1 - \iota)\right\}$, $k = 1,\ldots,n$, $\Gamma_2 = \min\left(2^{\frac{\iota+1}{2}}, 2^{\frac{\iota+1}{2}}\eta_k, \frac{\lambda_k}{(2\gamma_k)^{\frac{1-\iota}{2}}}, 2^{\frac{\iota+1}{2}}\right)$, $k = 1,\ldots,n$, and $C = \frac{1}{2}\sum_{k=1}^{n}\overline{\phi}_k^2 + \sum_{k=1}^{n}\frac{\lambda_k}{2\gamma_k}\theta_k^{*2} + \sum_{k=1}^{n-1}g_k\varpi_{k+1} + \sum_{k=1}^{n}\frac{\lambda_k(1-\iota)}{4\gamma_k} + \frac{(2n+1)(1-\iota)}{2}$.

From *Lemma 3*, the system (1) is SGPFS for $t \ge t_0 + T_c$. The finite-time convergence, T_c, is then determined as

$$T_c \le \max\left\{t_0 + \frac{1}{\lambda_0\Gamma_1\left(\frac{1-\iota}{2}\right)}\ln\frac{\lambda_0\Gamma_1 W^{\frac{1-\iota}{2}}(t_0) + \Gamma_2}{\Gamma_2}, t_0 + \frac{1}{\Gamma_1\left(\frac{1-\iota}{2}\right)}\ln\frac{\Gamma_1 W^{\frac{1-\iota}{2}}(t_0) + \lambda_0\Gamma_2}{\lambda_0\Gamma_2}\right\}. \tag{70}$$

with $0 < \lambda_0 < 1$ and the function $W_n(t)$ is bounded by:

$$\lim_{t\to T_c} W_n(t) \le \min\left\{\frac{C}{(1-\lambda_0)\Gamma_1}, \left(\frac{C}{(1-\lambda_0)\Gamma_2}\right)^{\frac{2}{\iota+1}}\right\}. \tag{71}$$

Therefore, the stability proof of the closed-loop system is completed.

Regarding the above proof, the closed-loop system stability is guaranteed if the control gains and observer gains satisfy the following conditions:

$$\begin{cases} 2\omega_k - 7 - \iota > 0 \\ \lambda_k(1-\iota) > 0 \\ \dfrac{\lambda_{\min}(\mathbf{Q})}{\sigma} - \| \mathbf{P} \|^2 - (\iota+1)\| \mathbf{P} \|^2 - \left(\overline{\omega}^2\left(2+\overline{g}^2\right)+\overline{\omega}^4\right) > 0 \\ 2(\kappa_k - 1) > 0 \\ 2\kappa_k - 1 - \iota > 0 \end{cases} \tag{72}$$

As seen, by setting suitable control and observer gains, the stability of the closed-loop system can be achieved. Theoretically, large values can help achieve fast response and convergence; however, this also brings a tradeoff of inducing unexpected chattering phenomenon and performance degradation due to the system's characteristics. Therefore, to avoid this problem encountered, these parameters should be carefully adjusted as the following:

- Set $\eta_k = 0$ and set arbitrary small values for κ_1 ($\kappa_1 > 1$ and $2\kappa_1 > 2 > 1 + \iota$) such that the output position can follow the desired trajectory. For k=2, …, n, theoretically, values of κ_k should be set smaller than κ_1.
- The Gaussian functions are selected based on the characteristics of the motion such as maximum movement, velocity, torque/force or inside dynamical behaviors. Set initial value $\widehat{\theta}_{k,0} > 0$. Noted that $\widehat{\theta}_{k+1,0} > \widehat{\theta}_{k,0}$ because the dynamical behaviors of the inner loop is faster than the outer loop.

- Set $\lambda_k = 0$ and gradually increase the learning rate γ_k from a very small value and check the convergence of the approximated $\widehat{\theta}_k$. Once light fluctuation occurs, stop tuning the learning rate γ_k and fix a value that is smaller than the current one. This helps prevent unexpected chattering because of the mutual influence of the approximation between the outer and inner loops.
- Slowly increase ω_k from $\omega_k > 0.5(7 + \iota)$ and check the tracking performance. Stop increasing ω_k when fluctuation is observed, or until the output tracking error has not much changed without chattering, then fix a value that is less than the current one. Besides, observer gains $l_k(\delta)/\sigma$ should be designed such that the matrix **A** in (25) satisfy Hurwitz. Thus, these gains were adopted through an observer bandwidth δ that depends on the order of the system.
- Slightly increase values of λ_k and check the system qualification. It is noted that this value should be less than γ_k. otherwise, the approximated $\widehat{\theta}_k$ may converge to non-optimal value.
- After achieving the above adjustment, slightly increase η_k and λ_k, but these should be maintained at small values, to enhance the tracking qualification.

5. Verification

In this section, comparative simulations on an electro-hydraulic system (EHS) is carried out with three controllers: (1) the proposed methodology, (2) a proportional-integral-derivative (PID) control, considered a specific model-free approach, and (3) an ideal model-based BSC, considered a benchmark model-based with all existing dynamical behaviors. The aim is to evaluate the effectiveness of the proposed methodology in achieving near the same tracking performance as the model-based with only output feedback to the main controller like the model-free approach. The system dynamics of the EHS is inheritably derived from [50] as

$$\begin{cases} \dot{x}_1 = x_2 \\ \dot{x}_2 = f_2 + g_2 x_3 + d_2 \\ \dot{x}_3 = f_3 + g_3 u + d_3 \end{cases}, \tag{73}$$

with $\mathbf{x} = (x_1, x_2, x_3)^T = (x \quad \dot{x} \quad A_1P_1 - A_2P_2)^T$, $g_2 = 1/m$, $d_2 = -F_{ext}/m$, $f_2 = (-b_1x_2 - b_2\tanh(b_3x_2))/m$, $f_3 = \left(-\frac{A_1^2}{V_1} - \frac{A_2^2}{V_2}\right)\beta x_2$, $d_3 = \left(-\frac{A_1}{V_1} - \frac{A_2}{V_2}\right)\beta q_L$, $q_L = C_t(P_1 - P_2)$, $g_3 = \left(\frac{A_1}{V_1}R_1 + \frac{A_2}{V_2}R_2\right)\beta k_t$, $k_t = C_d\omega k_v\sqrt{\frac{2}{\rho}}$, $V_1 = V_{10} + A_1x_1$, $R_1 = s(x_v)\sqrt{P_S - P_1} + s(-x_v)\sqrt{P_1 - P_t}$, $V_2 = V_{20} + A_2(L - x_1)$, $R_2 = s(x_v)\sqrt{P_2 - P_t} + s(-x_v)\sqrt{P_S - P_2}$. Herein, x and $\dot{x}$ are position and velocity of the end-effector; m is the total weight of the cylinder stroke and end-effector block; b_1 and b_2 are friction coefficients; d_2 stands for lumped matched uncertainty; A_1 and A_2 denote cross-section areas in bore-side and rod-side of the cylinder, respectively; L denotes the cylinder stroke; P_1 and P_2 are pressure in the bore-side and rod-side of the cylinder, respectively; V_1 and V_2 are volumes in the bore-side and rod-side, including initial volume of pipelines, V_{10} and V_{20}, of the cylinder, respectively; β denotes the Bulk modulus; k_t is the coefficient factor that presents the relationship between the control signal u and spool valve displacement x_v, i.e., $x_v = k_tu$; P_s and P_t denote supply and tank pressure, respectively; q_L is the simplified internal leakage model; and C_t is internal leakage coefficient.

The values of system parameters are followed from [50] with $L = 0.5$ (m); $A_1 = A_2 = 1.2\times10^{-4}$ (m^2); $m = 0.327$ (kg); $b_1 = 45$ (N/m/s); $b_2 = 0.01$ (N), $b_3 = 10^4$; $F_{ext} = 10$ (N); $\beta = 1.5\times10^9$ (Pa); $V_{10} = V_{20} = 1.15\times10^{-4}$ (m^3); $k_t = 2\times10^{-8}$ (m^3/s/V/$Pa^{1/2}$); $P_S = 100$ (bar); $P_t = 1$ (bar), $C_t = 1.8\times10^{-8}$ (m^3/s/Pa). Initial $x_1(t_0) = x_2(t_0) = x_v(t_0) = 0$, $P_1(t_0) = P_2(t_0) = 0$.

The aim is to track a reference motion, which is defined as

$$x_{1,d} = 0.25 + 0.2\sin(\pi t)\ (m). \tag{74}$$

The control parameters are as the followings:

PID: $K_P = 500$; $K_I = 10000$; $K_D = 0.01$,

BSC: $\kappa_1 = 500$; $\kappa_2 = 300$; $\kappa_3 = 1500$, $\eta_1 = 2$, $\eta_2 = 1$, $\eta_3 = 1$, $\iota = 3/5$,

Proposed: same control gains as the BSC; RBFNN structure: $\mathbf{c}_{f2} = [\mathbf{c}_{f21}, \mathbf{c}_{f22}]^T$ with $\mathbf{c}_{f21} = \mathbf{c}_{f22} = [-2, -1, 0, 1, 2]$; $\mathbf{c}_{f3} = [\mathbf{c}_{f31}, \mathbf{c}_{f32}, \mathbf{c}_{f33}]^T$ with $\mathbf{c}_{f31} = \mathbf{c}_{f32} = [-2, -1.5, -1, -0.5, 0, 0.5, 1, 1.5, 2]$; $\mathbf{c}_{f33} = 10^3 \times [-1, -0.75, -0.5, -0.25, 0, 0.25, 0.5, 0.75, 1]^T$, $\mu_{f2} = 2$, $\mu_{f3} = 20$, $\gamma_{f2} = 2\times10^3$; $\lambda_{f2} = 5\times10^{-4}$, $\gamma_{f3} = 2\times10^4$; $\lambda_{f3} = 5\times10^{-4}$; Initial weighting vectors: $\theta_{f2,0} = 10$, $\theta_{f3,0} = 2\times10^5$; NSDO: $\sigma = 1$, $\delta = 2000$, $l_1 = 3\delta$, $l_2 = 3\delta^2$, $l_3 = \delta^3$, $\omega_2 = 15$, $\omega_3 = 150$,

CF: $\varpi_{2,c} = \varpi_{3,c} = 10^{-4}$.

The NN-approximator architecture of the proposed control strategy in the second step includes two inputs of x_1 and $\hat{x}_2$ in the input layer, and five nodes in the hidden layer. In the third step, the NN is structured with three inputs of x_1, $\hat{x}_2$, and $\hat{x}_3$ in the input layer and nine nodes in the hidden layer.

Remark 5. For a fair comparison, controller gains of three comparative approaches should be equivalently selected. However, it is difficult to accomplish this because the executions of these methods are different, in essence, where one is a model-free and the other two are model-based techniques. Thus, the PID controller gains are heuristically designed to achieve the best tracking performance with less chattering in the output performance. The parameters of proposed method and BSC, followed by the guideline, are adopted as the same values as each other.

Remark 6. To facilitate the control expressions, the driver's dynamics is assumed to ideally operate without delay; thus, the control signal u is proportional to the spool valve displacement.

The system output qualification is pointed out in Fig. 2 in which the continuous black line represents the reference trajectory, the dotted-green line, the dotted-dashed-red line, and the dashed-blue line denote the output responses under the PID, model-based BSC, and proposed technique, respectively. The upper subfigure displays the output tracking performance while the bottom subfigure shows the output tracking error. As seen, the PID method offered the simplest implementation because only the actuator movement was feedback for the control execution; nevertheless, it returned the worst tracking qualification with the largest tracking error of $\pm 1.15\times 10^{-4}$ (m). Besides, at the beginning, significant fluctuation was generated. These drawbacks came from the uncompensated dynamical behaviors and the influence of the external disturbance F_{ext}. Increasing the PID gains could only improve the tracking effort, but they could not address the system dynamics and uncertainties, which had a significant influence. In contrast, the full-state feedback BSC achieved the best regulation with the smallest tracking error of approximately $\pm 2.5\times 10^{-5}$ (m) because all parameters of the system were available; thus, the dynamical behaviors was comprehensively compensated and the influence of the predefined disturbance was also suppressed. Meanwhile, although the proposed control methodology only required the feedback output signal, like the former PID, it could achieve nearly similar performance to the model-based approach. This result could be obtained because the system dynamics was approximated with the lumped disturbance and uncertainties estimated as presented through the norm estimation RBFNN-based approximation and NDSO. Thereby, these terms were suppressed in the virtual signals and control law executions. As a result, the influences of unstructured dynamics behaviors and uncertainties were relaxed and the tracking performance could be enhanced by only concerning the control gains κ_k.

Fig. 3 displays the system velocity, i.e., x_2, responses with the smallest error of PID in comparison with the other controllers. The reason is that the actuator velocity under the PID control was regulated through control gain K_D to follow the desired $\dot{x}_{1d}$. Meanwhile, the velocity under the BSC followed the virtual $x_{2d} = \dot{x}_{1d} - \kappa_1 s_1 - \eta_1 z_1^l$ and under the proposed method, $\hat{x}_2$, followed the virtual control $x_{2d} = \dot{x}_{1d} - \kappa_1 s_1 - \eta_1 z_1^l - \frac{l_1(\delta)}{\sigma}(y - \hat{x}_1)$ instead, not $\dot{x}_{1d}$ like the PID approach. Moreover, one can also observe the chattering in the velocity response under the PID technique. This came from the initial position $x(t_0)$, which was set far from reference and uncompensated dynamics when conducting the control execution.

Fig. 4 shows the response of the load force, i.e., state x3, in which the response under the proposed control nearly followed the model-based BSC. The control input signals are performed in Fig. 5. Generally, all control signals exerted fluctuations at the beginning because the initial position x(t0) was set at 0, which was far from the initial position of the reference. Thus, the control action executed more effort to regulate the current initial position to the reference one at the beginning, and over-shoot inevitably existed. However, the fluctuation under the PID was significant due to not considering the uncompensated disturbance, uncertainties, and dynamical behaviors, which had a significant effect on the output performance. On the contrary, the BSC generated the least fluctuation since all dynamics, disturbances, and uncertainties were compensated. The control action under the proposed technique quite fluctuated more than the model-based approach. This is reasonable because it required a certain time (finite time) for all unknown parameters and unstructured dynamics and uncertainties to be approximated by adaptive laws.

It is noteworthy that responses of velocity and load force under the proposed control scheme in Figs. 3 and 4 were of the estimated values because the states x_2 and x_3 were not available. The estimations of x_2 and x_3 are performed in Fig. 6, where the black line denotes the actual system state (obtained in the case when all system states are measurable) and the dot-dashed red line describes the estimated values. Generally, these results indicated that the NDSO could successfully estimate unavailable state variables for the proposed control implementation. Moreover, the actual load x_3 exerted severe chattering at the beginning because it was directly calculated from measured pressure, which was strongly affected by dynamical behaviors. Thus, this variable was vulnerable to chattering if the sampling time was not properly set, from the theory and simulation point of view, or if noise was not filtered out when

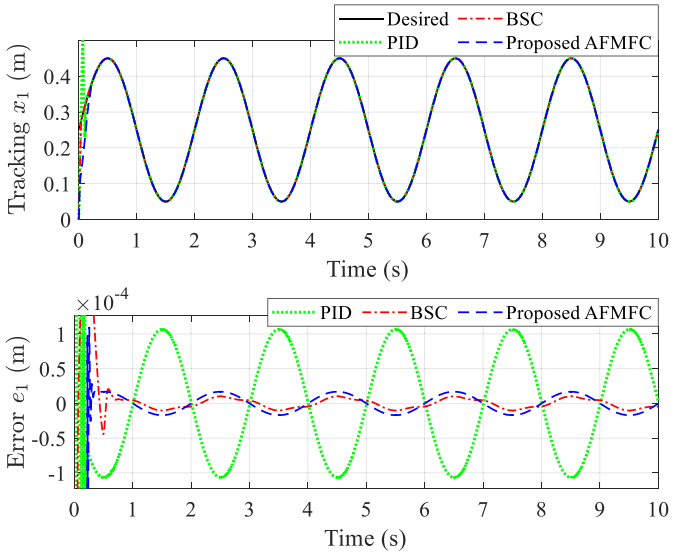

Fig. 2. Tracking effort of the system state x_1.

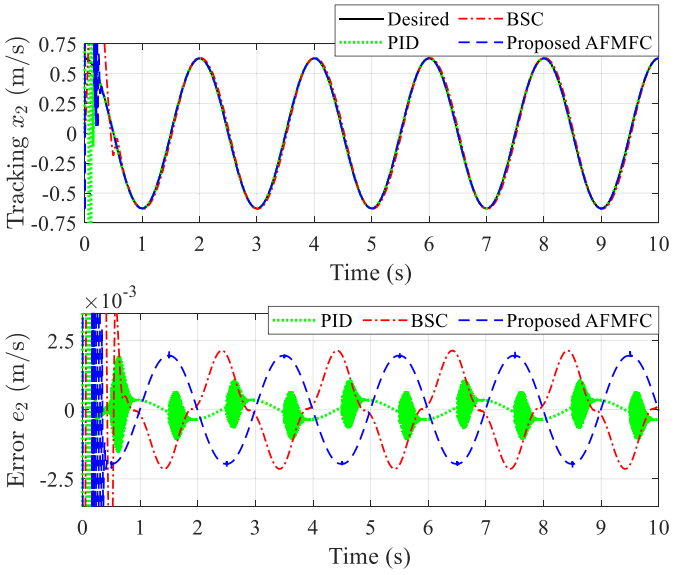

Fig. 3. Estimated and tracking effort of the system state x_2.

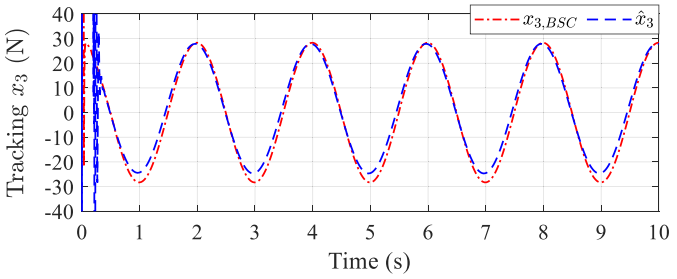

Fig. 4. Estimated and tracking effort of the system state x_3.

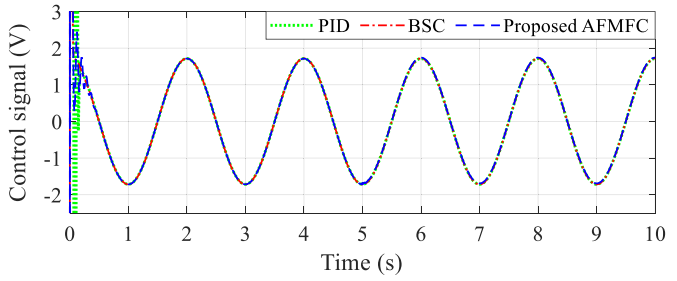

Fig. 5. Control input signal u under different methodologies.

using sensors to measure pressure when conducting experiments. On the contrary, the estimation performed a smoother response because it was obtained from the NDSO, where estimated parameters conventionally were smoothened out. However, inappropriate observer gains or sampling time could also deteriorate the observer qualification, in both simulation and practice.

The norm estimations of $\widehat{\theta}_2$ and $\widehat{\theta}_3$ are revealed in Fig. 7 with non-negative responses. Accordingly, the positive part $\widehat{f}_k(\widehat{\mathbf{x}}|\widehat{\overline{\mathbf{x}}}_k) = \frac{1}{2}\widehat{\theta}_k\boldsymbol{\varphi}_k^T(\widehat{\overline{\mathbf{x}}}_k)\boldsymbol{\varphi}_k(\widehat{\overline{\mathbf{x}}}_k)$, where $k = 2, 3$, are obtained as shown in Fig. 8, with continuous blue lines. As can be observed, due to using norm, these equivalent approximations always performed non-negative values and the norm estimations were stably adapted to the system behavior. However, in comparison to the original $f_k(\mathbf{x}) = \boldsymbol{\Xi}_k^{*T}\boldsymbol{\varphi}_k(\mathbf{x})$ that varied with both positive and negative values, to reflect the original behavior, the lumped ϕ_k were subsequently estimated that returned negative parts of $f_k(\mathbf{x})$, as shown in Fig. 8 with dot-dashed red color lines. As a result, the sum of $\widehat{f}_k(\widehat{\mathbf{x}}|\widehat{\overline{\mathbf{x}}}_k) = \frac{1}{2}\widehat{\theta}_k\boldsymbol{\varphi}_k^T(\widehat{\overline{\mathbf{x}}}_k)\boldsymbol{\varphi}_k(\widehat{\overline{\mathbf{x}}}_k)$ and $\widehat{\phi}_k$ reconstructed the behaviors of actual $f_k(\mathbf{x}) = \boldsymbol{\Xi}_k^{*T}\boldsymbol{\varphi}_k(\mathbf{x})$ in the right way.

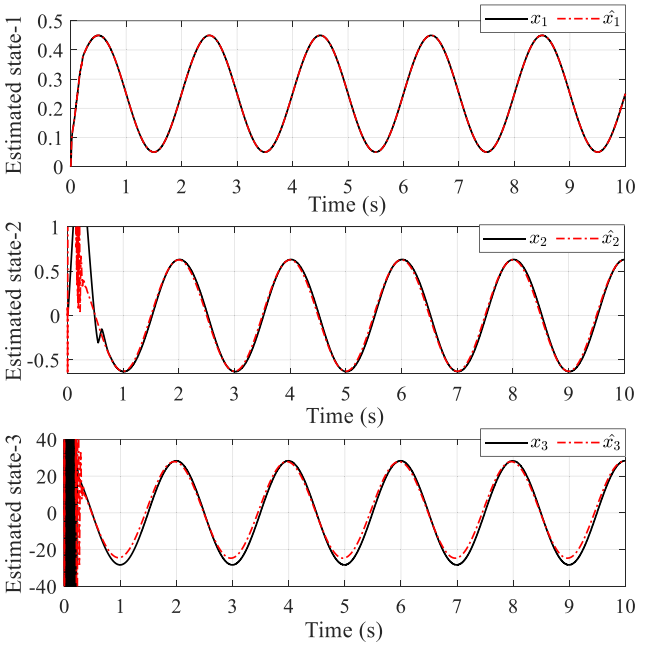

Fig. 6. Comparison between the actual and estimated state.

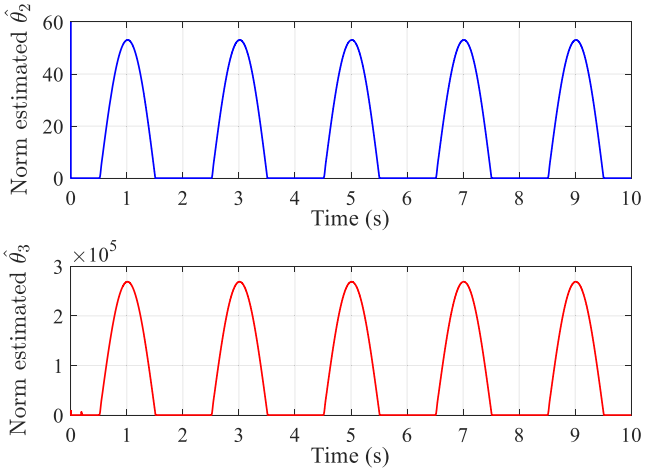

Fig. 7. Norm estimation of $\widehat{\theta}_2$ and $\widehat{\theta}_3$.

As can be said that our idea is decoupling the dynamics $\boldsymbol{\Xi}_k^{*T}\boldsymbol{\varphi}_k(\mathbf{x})$ into two positive and negative parts. The positive part was performed by using RFBNN with norm estimation, while the negative part was obtained by estimating ϕ_k. Thus, instead of updating all 14 parameters (5 nodes of $\widehat{\Xi}_2 = (\widehat{\xi}_{2,1}\ \widehat{\xi}_{2,2}\ \ldots\ \widehat{\xi}_{2,5})^T$for approximating $\boldsymbol{\Xi}_2^{*T}\boldsymbol{\varphi}_2(\mathbf{x}|\widehat{\mathbf{x}}_2)$ and 9 nodes of $\widehat{\Xi}_3 = (\widehat{\xi}_{3,1}\ \widehat{\xi}_{3,2}\ \ldots\ \widehat{\xi}_{3,9})^T$ for approximating $\boldsymbol{\Xi}_3^{*T}\boldsymbol{\varphi}_3(\hat{\mathbf{x}})$), only 2 parameters to be updated, i.e., $\widehat{\theta}_2 = \|\ \widehat{\Xi}_2\|^2$ and $\widehat{\theta}_3 = \|\ \widehat{\Xi}_3\|^2$. As a results, less updated parameters reduced the computation cost with less time-consuming, especially when extending to other applications such as an ESS with servo-valve dynamics included, where a fourth- or fifth-order system is modeled, or when the dynamics of a driver is taken into the automatic systems modeling.

Furthermore, in the simulation, the initial value of $W(t_0)$ depends on tracking position error, initial estimation error, control, and observer gains at the initial time $t_0 = 0$. Thus, based on the values selected for the simulation, one can obtain the finite time T_c. However, it is not easy to obtain these errors because we cannot know exactly the value of optimal norm $\theta_k^* = \|\ \boldsymbol{\Xi}_k^*\|^2$ (or optimal weighting vector. But we know the initial value $\widehat{\theta}_k(t_0)$ based on the value set in the simulation), and W_0 at t_0=0; thus, $W(t_0)$ cannot be exactly obtained. In our evaluation, we assumed that at the initial time, the estimation errors are all zero, i.e., $\varepsilon_k = \phi_k = \widetilde{\theta}_k = \zeta_k = 0$, except for the tracking errors of the position $s_1(t_0) = x_1(t_0) - x_{1,\mathrm{d}}(t_0)$ and velocity $s_2(t_0) = x_2(t_0) - x_{2,\mathrm{c}}(t_0)$ since $x_{1,\mathrm{d}}(t_0) = 0.25$ [m] and $x_{2,}$

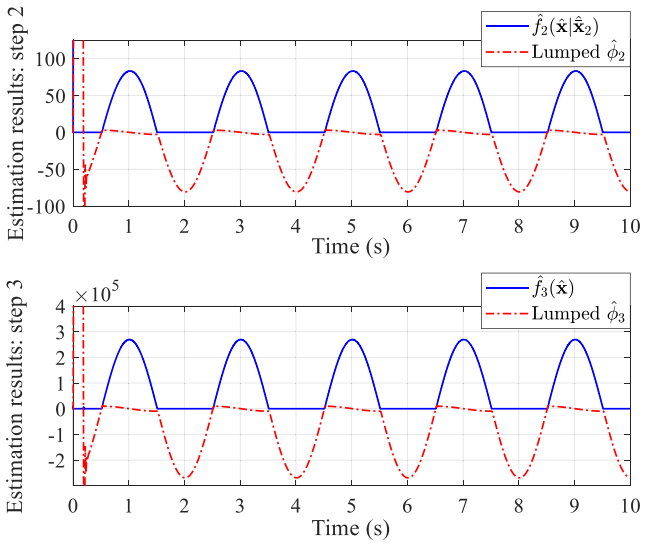

Fig. 8. Positive part $\widehat{f}_k(\hat{\mathbf{x}}|\widehat{\hat{\mathbf{x}}}_k) = \frac{1}{2}\widehat{\theta}_k\boldsymbol{\varphi}_k^T(\widehat{\hat{\mathbf{x}}}_k)\boldsymbol{\varphi}_k(\widehat{\hat{\mathbf{x}}}_k)$ of $\boldsymbol{\Xi}_k^{*T}\boldsymbol{\varphi}_k(\mathbf{x})$, and estimated lumped $\widehat{\phi}_k$.

$_c(t_0) = x_{2,d}(t_0) = 0.25 + 0.2\pi$ [m/s]. g_2 and g_3, relating to the stability of the NDSO, can also be obtained based on their formulas. Thereby, the initial $W(t_0)$ was much less than its actual initial value. Subsequently, one can obtain that the convergence time T_c is much less than the theoretical calculation, i.e., $T_c \ll \max\left\{t_0 + \frac{1}{\lambda_0\Gamma_1\left(\frac{1-l}{2}\right)}\ln\frac{\lambda_0\Gamma_1 W^{\frac{1-l}{2}}(t_0)+\Gamma_2}{\Gamma_2}, t_0 + \frac{1}{\Gamma_1\left(\frac{1-l}{2}\right)}\ln\frac{\Gamma_1 W^{\frac{1-l}{2}}(t_0)+\lambda_0\Gamma_2}{\lambda_0\Gamma_2}\right\}$ based on the control parameters, learning rates, and observer gains selection. Consequently, the justification of the practical finite-time stable was proven.

However, also obtained from Fig. 9, the approximated results did not accurately follow the actual dynamics $\boldsymbol{\Xi}_k^{*T}\boldsymbol{\varphi}_k(\mathbf{x})$. Moreover, although the proposed method can help reduce a number of estimated elements of the weighting vector and facilitate the advanced techniques integrated, there still exist shortcomings as the followings:

1) Compared to the actual dynamical behaviors f_k, the positive part of f_k was presented through $\widehat{f}_k(\widehat{\hat{\mathbf{x}}}_k)$ as they were approximated based on the system states, but ϕ_k included not only a negative part of f_k but also mismatched and matched disturbances/uncertainties, i.e., d_2 and d_3 in the simulation. It should be noted that for the case of unknown system dynamics, the influences of f_k are always lumped with disturbances and/or uncertainties because they appear in the same channel and are coupled with each other. Thereby, the approximation will return their lumped effect. This will certainly occur if mismatched and/or matched uncertainties are also functions of system states, i.e., internal leakage in this case study. However, if the system is only required to satisfy position

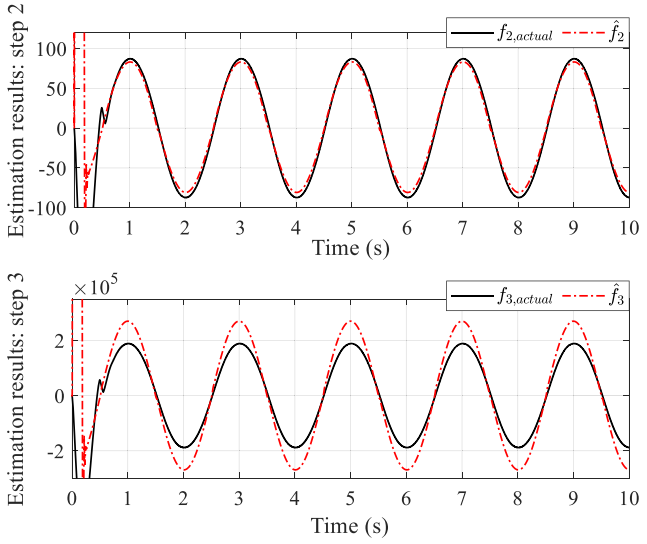

Fig. 9. Results of approximated unknown functions f_2 and f_3 in comparison with the real ones.

requirements, this issue cannot be ignored because the lumped dynamics are estimated and compensated by control laws implementation.

2) The parameters adopted for output tracking regulation, states estimation, and adaptive law for updating the estimated norms, have mutual influences. It is difficult to select optimal values for all variables. Then, how to achieve optimal solutions will become our next goal.
3) Due to using norm, the choice of the Gaussian basis function (centers and widths) becomes more significant where inappropriate design certainly affects the approximation accuracy. This does not appear on the conventional fuzzy logic or RRBFNN techniques owing to the flexibility in separately updating each element $\xi_{k,j(j=1,\ldots,N_k)}$ of the weighting vector $\boldsymbol{\Xi}_k^* = \begin{pmatrix} \xi_{k,1} & \xi_{k,2} & \cdots & \xi_{k,N_k} \end{pmatrix}^T \in \mathbb{R}^{N_k}$. Subsequently, the effect of inappropriate $\varphi_{k,j}$ (and corresponding center $\mathbf{c}_{k,j}$) is mitigated. This cannot be executed by using the norm estimation $\theta_k^* = \| \boldsymbol{\Xi}_k^* \|^2$ since $\xi_{k,j(j=1,\ldots,N_k)}$ cannot be extracted. Therefore, establishing or optimizing Gaussian basis function of self-organized RBF-based approximation evokes a new challenge to enhance the approximation and system performance.

6. Conclusion

With the output tracking requirement subject to partially unknown dynamics and unavailability of the system states, except for the measurable output only, this paper proposed a new methodology to not only address these difficulties but also achieve and improve the output tracking regulation. The proposed control scheme was constructed based on the RBFNN-norm estimation technique to cope with unstructured dynamical behavior. In order to make this approach implementable in the case of missing system state variables, the system was reformulated in which the unstructured dynamics term was presented in a new form of the RBFNN operator but still kept the same key properties as the original model. As the new form, the process errors, lumped into disturbance and uncertainties, consequently arose. Therefore, the NSDO was employed for not only state observation but also for lumped uncertainties and disturbances rejection to enhance the output tracking effort. Besides, the CF technique was also combined to obtain smooth virtual controls and their first derivatives as the requirement when deploying BSC. The stability of the closed-loop system was mathematically proven to guarantee that all signals were bounded and converged to the vicinity of the boundary in finite time. The effectiveness of the proposed control scheme was verified through comparative simulations. With the new approach using NN-based approximator, other advanced techniques, such as input saturation, input quantization, dead zone, state constraints, compliance control, and so on, can possibly be investigated, as future developments, to enhance the system qualification.

Data availability

No data was used for the research described in the article.

Acknowledgements

This work was supported by Korea Hydro & Nuclear Power Co and Ulsan (2023) and “Regional Innovation Strategy (RIS)” through the National Research Foundation of Korea (NRF) funded by the Ministry of Education (MOE) (2021RIS-003).

References

[1] S. Ullah, A. Mehmood, Q. Khan, S. Rehman, J. Iqbal, Robust integral sliding mode control design for stability enhancement of under-actuated quadcopter, Int. J. Control Autom. Syst. 18 (2020) 1671–1678, https://doi.org/10.1007/s12555-019-0302-3.
[2] S. Li, T. Ma, X. Lou, Z. Yang, Adaptive fuzzy output regulation for unmanned surface vehicles with prescribed performance, Int. J. Control Autom. Syst. 18 (2020) 405–414, https://doi.org/10.1007/s12555-019-0082-9.
[3] K. Eliker, W. Zhang, Finite-time adaptive integral backstepping fast terminal sliding mode control application on quadrotor UAV, Int. J. Control Autom. Syst. 18 (2020) 415–430.
[4] W. Zeng, Z. Li, C. Gao, L. Wu, Observer-based adaptive fuzzy control for strict-feedback nonlinear systems with prescribed performance and dead zone, Int. J. Control Autom. Syst. 19 (2021) 1962–1975, https://doi.org/10.1007/s12555-020-0245-8.
[5] W. Xu, Z. Li, G. Cui, F. Hu, Fuzzy adaptive finite time command filter backstepping control of power system, Int. J. Control Autom. Syst. 19 (2021) 3812–3822, https://doi.org/10.1007/s12555-020-0466-x.
[6] S. Li, T. Ma, X. Luo, Z. Yang, Adaptive fuzzy output regulation for unmanned surface vehicles with prescribed performance, Int. J. Control Autom. Syst. 18 (2020) 405–414, https://doi.org/10.1007/s12555-019-0082-9.
[7] D.T. Tran, X.B. Dang, K.K. Ahn, Adaptive backstepping sliding mode control for equilibrium position tracking of an electrohydraulic elastic manipulator, IEEE Trans. Ind. Electron. 67 (2020) 3860–3869, https://doi.org/10.1109/TIE.2019.2918475.
[8] D.T. Tran, H.V.A. Truong, K.K. Ahn, Adaptive backstepping sliding mode control based RBFNN for a hydraulic manipulator including actuator dynamics, Appl. Sci. 9 (2019) 1265, https://doi.org/10.3390/app9061265.
[9] W. Deng, J. Yao, Extended-state-observer-based adaptive control of electrohydraulic servomechanisms without velocity measurement, IEEE ASME Trans. Mechatron. 25 (2020) 1151–1161, https://doi.org/10.1109/TMECH.2019.2959297.
[10] J. Yao, Z. Jiao, D. Ma, Extended-state-observer-based output feedback nonlinear robust control of hydraulic systems with backstepping, IEEE Trans. Ind. Electron. 61 (2014) 6285–6293, https://doi.org/10.1109/TIE.2014.2304912.
[11] X. Yang, J. Yao, W. Deng, Output feedback adaptive super-twisting sliding mode control of hydraulic systems with disturbance compensation, ISA Trans. 109 (2021) 175–185, https://doi.org/10.1016/j.isatra.2020.09.014.
[12] G. Yang, J. Yao, Output feedback control of electro-hydraulic servo actuators with matched and mismatched disturbances rejection, J. Frankl. Inst. 356 (2019) 9152–9179, https://doi.org/10.1016/j.jfranklin.2019.07.032.
[13] J. Yao, W. Deng, Active disturbance rejection adaptive control of uncertain nonlinear systems: theory and application, Nonlinear Dyn. 89 (2017) 1611–1624, https://doi.org/10.1007/s11071-017-3538-6.

[14] Z. Yao, J. Yao, W. Sun, Adaptive RISE control of hydraulic systems with multilayer neural-networks, IEEE Trans. Ind. Electron. 66 (2019) 8638–8647, https://doi.org/10.1109/TIE.2018.2886773.

[15] D.X. Ba, T.Q. Dinh, K.K. Ahn, An integrated intelligent nonlinear control method for a pneumatic artificial muscle, IEEE ASME Trans. Mechatron. 21 (2016) 1835–1845, https://doi.org/10.1109/TMECH.2016.2558292.

[16] M.D. Tran, H.J. Kang, Adaptive terminal sliding mode control of uncertain robotic manipulators based on local approximation of a dynamic system, Neurocomputing 228 (2017) 231–240, https://doi.org/10.1016/j.neucom.2016.09.089.

[17] D.T. Tran, H.V.A. Truong, K.K. Ahn, Adaptive nonsingular fast terminal sliding mode control of robotic manipulator based neural network approach, Int. J. Precis. Eng. Manuf. 22 (2021) 417–429, https://doi.org/10.1007/s12541-020-00427-4.

[18] W. He, Y. Sun, Z. Yan, C. Yang, Z. Li, O. Kaynak, Disturbance observer-based neural network control of cooperative multiple manipulators with input saturation, IEEE Trans. Neural Netw. Learn. Syst. 31 (2020) 1735–1746, https://doi.org/10.1109/TNNLS.2019.2923241.

[19] C. Wu, J. Liu, Y. Xiong, L. Wu, Observer-based adaptive fault-tolerant tracking control of nonlinear nonstrict-feedback systems, IEEE Trans. Neural Netw. Learn. Syst. 29 (2018) 3022–3033, https://doi.org/10.1109/TNNLS.2017.2712619.

[20] Y. Xu, Q. Zhou, T. Li, H. Liang, Event-triggered neural control for non-strict-feedback systems with actuator failures, IET Control Theory Appl. 13 (2019) 171–182, https://doi.org/10.1049/iet-cta.2018.5403.

[21] C. Zhang, G. Yang, Event-triggered adaptive output feedback control for a class of uncertain nonlinear systems with actuator failures, IEEE Trans. Cybern. 50 (2020) 201–210, https://doi.org/10.1109/TCYB.2018.2868169.

[22] J. Zhang, S. Tong, Adaptive fuzzy output feedback FTC for nonstrict-feedback systems with sensor faults and dead zone input, Neurocomputing 435 (2021) 67–76, https://doi.org/10.1016/j.neucom.2021.01.008.

[23] W. Sun, L. Wang, Y. Wu, Adaptive dynamic surface fuzzy control for state constrained time-delay nonlinear nonstrict feedback systems with unknown control directions, IEEE Trans. Syst. Man Cybern. Syst. 51 (2021) 7423–7434, https://doi.org/10.1109/TSMC.2020.2969289.

[24] J. Yu, P. Shi, W. Dong, C. Lin, Adaptive fuzzy control of nonlinear systems with unknown dead zones based on command filtering, IEEE Trans. Fuzzy Syst. 16 (2018) 46–55, https://doi.org/10.1109/TFUZZ.2016.2634162.

[25] B. Cao, X. Nie, Z. Wu, C. Xue, J. Cao, Adaptive neural network control for nonstrict-feedback uncertain nonlinear systems with input delay and asymmetric time-varying state constraints, J. Frankl. Inst. 358 (2021) 7073–7095, https://doi.org/10.1016/j.jfranklin.2021.07.020.

[26] Y. Liu, H. Zhang, Y. Wang, S. Sun, Adaptive fuzzy control for nonstrict-feedback systems under asymmetric time-varying full state constraints without feasibility condition, IEEE Trans. Fuzzy Syst. 29 (2021) 976–985, https://doi.org/10.1109/TFUZZ.2020.2965908.

[27] S. Wang, J. Xia X. Wang, W. Yang, L. Wang, Adaptive neural networks control for MIMO nonlinear systems with unmeasured states and unmodeled dynamics, Appl. Math. Comput. 408 (2021) 126369, https://doi.org/10.1016/j.amc.2021.126369.

[28] Y. Wang, J. Zhang, H. Zhang, X. Xie, Finite-time adaptive neural control for nonstrict-feedback stochastic nonlinear systems with input delay and output constraints, Appl. Math. Comput. 393 (2021) 125756, https://doi.org/10.1016/j.amc.2020.125756.

[29] W. Bi, T. Wang, Adaptive fuzzy decentralized control for nonstrict feedback nonlinear systems with unmodeled dynamics, IEEE Trans. Syst. Man Cybern. Syst. 52 (2022) 275–286, https://doi.org/10.1109/TSMC.2020.2997703.

[30] J. Zhang, S.C. Tong, Y.M. Li, Adaptive fuzzy finite-time output-feedback fault-tolerant control of nonstrict-feedback systems against actuator faults, IEEE Trans. Syst. Man Cybern. Syst. 52 (2022) 1276–1287, https://doi.org/10.1109/TSMC.2020.3011702.

[31] D.Y. Jin, B. Niu, H.Q. Wang, D. Yang, A new adaptive ds-based finite-time neural tracking control scheme for nonstrict-feedback nonlinear systems, IEEE Trans. Syst. Man Cybern. Syst. 52 (2022) 1014–1018, https://doi.org/10.1109/TSMC.2020.3009405.

[32] G. Cui, J. Yu, P. Shi, Observer-based finite-time adaptive fuzzy control with prescribed performance for nonstrict-feedback nonlinear systems, IEEE Trans. Fuzzy Syst. 30 (2022) 767–778, https://doi.org/10.1109/TFUZZ.2020.3048518.

[33] S. Kamali, S.M. Tabatabaei, M.M. Arefi, S. Yin, Prescribed performance quantized tracking control for a class of delayed switched nonlinear systems with actuator hysteresis using a filter-connected switched hysteretic quantizer, IEEE Trans. Neural Netw. Learn. Syst. 33 (2022) 61–74, https://doi.org/10.1109/TNNLS.2020.3027492.

[34] D. Wu, Y. Sun, R. Xia, S. Lu, Improved adaptive fuzzy control for non-strict feedback nonlinear systems: a dynamic compensation system approach, Appl. Math. Comput. 435 (2022) 127470, https://doi.org/10.1016/j.amc.2022.127470.

[35] Z. Wu, T. Zhang, X. Xia, Y. Hua, Finite-time adaptive neural command filtered control for non-strict feedback uncertain multi-agent systems including prescribed performance and input nonlinearities, Appl. Math. Comput. 421 (2022) 126953, https://doi.org/10.1016/j.amc.2022.126953.

[36] J. Qiu, T. Wang, K. Sun, I.J. Rudas, H. Gao, Disturbance observer-based adaptive fuzzy control for strict-feedback nonlinear systems with finite-time prescribed performance, IEEE Trans. Fuzzy Syst. 30 (2022) 1175–1185, https://doi.org/10.1109/TFUZZ.2021.3053327.

[37] J. Qiu, K. Sun, I.J. Rudas, H. Gao, Command filter-based adaptive NN control for MIMO nonlinear systems with full-state constraints and actuator hysteresis, IEEE Trans. Cybern. 50 (2020) 2905–2915, https://doi.org/10.1109/TCYB.2019.2944761.

[38] J. Xia, J. Zhang, J. Feng, Z. Wang, G. Zhuang, Command filter-based adaptive fuzzy control for nonlinear systems with unknown control directions, IEEE Trans. Syst. Man Cybern. Syst. 51 (2021) 1945–1953, https://doi.org/10.1109/TSMC.2019.2911115.

[39] S. Tong, Y. Li, S. Sui, Adaptive fuzzy tracking control design for SISO uncertain nonstrict feedback nonlinear systems, IEEE Trans. Fuzzy Syst. 24 (2016) 1441–1454, https://doi.org/10.1109/TFUZZ.2016.2540058.

[40] L. Ma, L. Liu, Adaptive neural network control design for uncertain nonstrict feedback nonlinear system with state constraints, IEEE Trans. Syst. Man Cybern. Syst. 51 (2021) 3678–3686, https://doi.org/10.1109/TSMC.2019.2922393.

[41] K. Sun, J. Qiu, H.R. Karimi, H. Gao, A novel finite-time control for nonstrict feedback saturated nonlinear systems with tracking error constraint, IEEE Trans. Syst. Man Cybern. Syst. 51 (2021) 3968–3979, https://doi.org/10.1109/TSMC.2019.2958072.

[42] J.D. Liu, B. Niu, Y.G. Kao, P. Zhao, D. Yang, Decentralized adaptive command filtered neural tracking control of large-scale nonlinear systems: an almost fast finite-time framework, IEEE Trans. Neural Netw. Learn. Syst. 32 (2021) 3621–3632, https://doi.org/10.1109/TNNLS.2020.3015847.

[43] J. Yu, P. Shi, L. Zhao, Finite-time command filtered backstepping control for a class of nonlinear systems, Automatica 92 (2018) 173–180, https://doi.org/10.1016/j.automatica.2018.03.033.

[44] C.M. Ho, D.T. Tran, C.H. Nguyen, K.K. Ahn, Adaptive neural command filtered control for pneumatic active suspension with prescribed performance and input saturation, IEEE Access 9 (2021) 56855–56868, https://doi.org/10.1109/ACCESS.2021.3071322.

[45] J. Qiu, K. Sun, I.J. Rudas, H. Gao, Command filter-based adaptive NN control for MIMO nonlinear systems with full-state constraints and actuator hysteresis, IEEE Trans. Cybern. 50 (2020) 2905–2915, https://doi.org/10.1109/TCYB.2019.2944761.

[46] S. Li, C.K. Ahn, Z. Xiang, Command-filter-based adaptive fuzzy finite-time control for switched nonlinear systems using statedependent switching method, IEEE Trans. Fuzzy Syst. 29 (2021) 833–845, https://doi.org/10.1109/TFUZZ.2020.2965917.

[47] Y. Sun, B. Chen, C. Lin, H. Wang, S. Zhou, Adaptive neural control for a class of stochastic nonlinear systems by backstepping approach, Inf. Sci. 369 (2016) 748–764.

[48] M. Chen, S.S. Ge, Adaptive neural output feedback control of uncertain nonlinear systems with unknown hysteresis using disturbance observer, IEEE Trans. Ind. Electron. 62 (2015) 7706–7716, https://doi.org/10.1109/TIE.2015.2455053.

[49] H.V.A. Truong, H.A. Trinh, D.T. Tran, K.K. Ahn, A robust observer for sensor faults estimation on n-DOF manipulator in constrained framework environment, IEEE Access 9 (2021) 88439–88451, https://doi.org/10.1109/ACCESS.2021.3087505.

[50] V.D. Phan, C.P. Vo, H.V. Dao, K.K. Ahn, Actuator fault-tolerant control for an electro-hydraulic actuator using time delay estimation and feedback linearization, IEEE Access 9 (2021) 107111–107123, https://doi.org/10.1109/ACCESS.2021.3101038.